

Optimal Binary Signaling for a Two Sensor Gaussian MAC Network

Luca Sardellitti¹, Glen Takahara, *Member, IEEE*, and Fady Alajaji², *Senior Member, IEEE*

Abstract—We consider a two sensor distributed detection system transmitting a binary non-uniform source over a Gaussian multiple access channel (MAC). We model the network via binary sensors whose outputs are generated by binary symmetric channels of different noise levels. We prove an optimal one dimensional constellation design under individual sensor power constraints which minimizes the error probability of detecting the source. Three distinct cases arise for this optimization based on the parameters in the problem setup. In the most notable case (Case III), the optimal signaling design is to not necessarily use all of the power allocated to the more noisy sensor (with less correlation to the source). We compare the error performance of the optimal one dimensional constellation to orthogonal signaling. The results show that the optimal one dimensional constellation achieves lower error probability than using orthogonal channels.

Index Terms—Distributed detection, wireless sensor networks, multiple access channel, constellation design, binary signaling, power allocation, source-channel signaling, error probability.

I. INTRODUCTION

WIRELESS sensor networks are widely used for monitoring the state of real world phenomena. This includes both the estimation of a real valued parameter (such as temperature or rain fall measurements) and the detection of an event occurring (such as the occurrence of forest fires or a security breach). In this paper, we focus on the hypothesis testing problem described by distributed detection of an event occurring.

When working with generalized distributed detection problems, the error probability of the system cannot in general be expressed analytically. As a result, previous work on distributed detection typically uses related or proxy metrics for system error analysis. For example, [2] uses error exponents to evaluate the performance of various detection schemes, [3] uses the J-divergence (i.e., the Jeffreys-divergence [4]), while [5] and [6] use the deflection coefficient as the metric for optimization.

Previous work in this area employs a variety of signaling structures for the sensors. For example, [3] uses orthogonal channels for each sensor, while [6] uses a single MAC for

the entire network. Works such as [6], [7], [8], and [9] fix a signaling design and analyze detection schemes at the fusion center. Other works optimize the sensors' signaling techniques under certain constraints. For example, [3] optimizes power allocation for a network that uses orthogonal signaling and on-off keying for each sensor, under total and average power constraints. Alternatively, [5] assumes fixed power at each sensor, and analyzes the optimal rotation angle to send the signals. In [10], the problem of distributed mean-squared error estimation of a Gaussian source sent over a symmetric Gaussian sensor network is analyzed; it is shown that uncoded transmission (scalar coding) is optimal in the sense that it achieves Shannon's optimal performance theoretically achievable among all source-channel block codes of sufficiently large lengths. The distributed detection setup in this paper can be seen as a discretization of the distributed estimation system in [10] if we use a uniformly distributed source and symmetric sensor channels. The source and sensor readings can be represented as one bit quantizations of their continuous counterparts in [10]. Further, [11] extends the distributed estimation problem of [10] to include fading and asymmetric sensors, providing a sufficient condition under which uncoded transmission is optimal.

Throughout the above mentioned works, there is not much emphasis put on generalized constellation design for distributed detection problems. We aim to solve the source-channel signaling problem of finding an optimized constellation design to minimize error probability under a given source and channel model. This is similar in principle to works such as [12], [13], [14], [15], [16], [17], [18], [19], and [20], where general constellation design is optimized for a chosen criterion. In [12], the optimal joint binary constellation design for two correlated sources was derived. In [13] and [14], the authors used a minimum inter-constellation distance criterion for optimizing constellations for multiple sources. In contrast, [17], [18], [19], [20] optimized M -ary constellations for a single source. In this paper, we adapt these ideas to optimize signaling for a distributed detection system.

We simplify the distributed detection problem to a two sensor communication network so that an analytical optimization of the error probability can be performed. We model hypothesis testing for an event of interest occurring as a non-uniformly distributed binary source, and the sensor noises are modelled as passing the source through independent memoryless binary symmetric channels, introducing sensor errors. Finally, the sensors choose binary constellations to send their signals over a Gaussian MAC to the fusion center, which then performs the maximum-a-posteriori (MAP) detection

Manuscript received 6 February 2024; revised 5 June 2024; accepted 18 July 2024. Date of publication 29 July 2024; date of current version 16 January 2025. This work was supported in part by the Natural Sciences and Engineering Research Council (NSERC) of Canada. This work will be presented in part at the IEEE Canadian Conference of Electrical and Computer Engineering, Kingston, ON, Canada, August 2024 [1]. The associate editor coordinating the review of this article and approving it for publication was Y.-C. Huang. (Corresponding author: Luca Sardellitti.)

The authors are with the Department of Mathematics and Statistics, Queen's University, Kingston, ON K7L 3N6, Canada (e-mail: 16ls53@queensu.ca; takahara@queensu.ca; fa@queensu.ca).

Digital Object Identifier 10.1109/TCOMM.2024.3435404

0090-6778 © 2024 IEEE. Personal use is permitted, but republication/redistribution requires IEEE permission.
See <https://www.ieee.org/publications/rights/index.html> for more information.

rule to recover the source. With this setup, we analytically derive an optimal one dimensional constellation design to minimize the system error probability under individual power constraints for each sensor. The proof is split into three cases, based on the parameters describing the source distribution and sensors' noise. The constellation design is optimized in each of these cases using indirect analysis of the decision boundaries, followed by algebraic and derivative analysis using an upper bound on the error probability. In addition, we show using numerical and simulation results that the derived optimal one dimensional constellation achieves lower error probability than using orthogonal channels. Our most notable result is that in certain cases (which is dominant when the source is nearly uniformly distributed), the noisier sensor should use some but not all of its allocated power.

The rest of the paper is structured as follows. Section II describes the mathematical model of the sensor network, including the fusion center detection rule. Sections III and IV give a summary and a detailed proof of the main optimization results, respectively. Section V presents simulations and numerical examples which reinforce and illustrate the theoretically established results. Finally, Section VI draws conclusions and suggests future research directions.

II. SYSTEM MODEL

A. Source and Sensors

Let X be a binary event that is to be observed by a sensor network. Without loss of generality, it is assumed that the source is distributed such that $p_1 \triangleq \Pr(X = 1) \leq 0.5$. We also define $p_0 \triangleq \Pr(X = 0) = 1 - p_1$. There are two sensors, X_1 and X_2 observing the source X , which are modelled as passing X through two memoryless binary symmetric channels. This is expressed as $X_s = X \oplus Z_s$, $s = 1, 2$, where \oplus denotes addition modulo-2, with Z_1 and Z_2 being independent Bernoulli noise processes with means (or channel crossover probabilities) ϵ_1 and ϵ_2 , respectively. It is also assumed that X is independent from (Z_1, Z_2) . Without loss of generality, Sensor 1 is assumed to have stronger correlation to the original source X than Sensor 2: $0 < \epsilon_1 \leq \epsilon_2 < 0.5$. The sensors, unable to communicate with each other, encode their data independently using binary constellations. The constellations for the sensors are represented as follows: $\mathcal{C}_s = \{c_{0,s}, c_{1,s}\}$, $s \in \{1, 2\}$, where for $i \in \{0, 1\}$, $c_{i,s} \in \mathbb{R}$ denotes the constellation point for sensor s assigned to $X_s = i$. Let $S_1 \in \mathcal{C}_1$, $S_2 \in \mathcal{C}_2$ be the random variables associated to each sensor's chosen constellation point. Also let P_1^{\max} and P_2^{\max} be the power constraints of sensors, i.e., $E[S_i^2] \leq P_i^{\max}$, $i \in \{1, 2\}$. In this setup, each sensor has its own power allotment, as opposed to having a common power constraint on the entire network.

B. Channel Model

The sensors' signals are sent through a Gaussian MAC. The received signal R is described by the relation $R = S_1 + S_2 + Z$, where Z is a Gaussian noise variable with zero mean and variance $\frac{N_0}{2}$. For convenience, we also define σ as the standard deviation of the noise, given by $\sigma = \sqrt{\frac{N_0}{2}}$. It is assumed that

TABLE I
CASE CHARACTERIZATION CONDITIONS

Case	Condition	\mathcal{D}_0
I	$0 \leq p_1 \leq \frac{\epsilon_1 \epsilon_2}{1 - \epsilon_1 - \epsilon_2 + 2\epsilon_1 \epsilon_2}$	\mathbb{R}
II	$\frac{\epsilon_1 \epsilon_2}{1 - \epsilon_1 - \epsilon_2 + 2\epsilon_1 \epsilon_2} < p_1 \leq \frac{\epsilon_1 - \epsilon_1 \epsilon_2}{\epsilon_1 + \epsilon_2 - 2\epsilon_1 \epsilon_2}$	$(-\infty, x^*]$
III	$\frac{\epsilon_1 - \epsilon_1 \epsilon_2}{\epsilon_1 + \epsilon_2 - 2\epsilon_1 \epsilon_2} < p_1 \leq 0.5$	$(-\infty, x^*]$

Z is independent of the sensor signals S_1 and S_2 . The overall signal $S_1 + S_2$ sent over the channel can be represented as a point in the combined constellation of \mathcal{C}_1 and \mathcal{C}_2 , given by $\mathcal{C} = \{c_1 + c_2 \mid c_1 \in \mathcal{C}_1, c_2 \in \mathcal{C}_2\}$.

C. Maximum-a-Posteriori Detection

The event X is reconstructed at the fusion center using (optimal) MAP detection. For a Gaussian MAC received signal r , the detected bit is determined as follows:

$$\begin{aligned} \hat{x}(r) &= \arg \max_{i \in \{0,1\}} \Pr(X = i \mid R = r) \\ &= \arg \max_{i \in \{0,1\}} \Pr(X = i) f_R(r \mid X = i) \\ &= \arg \max_{i \in \{0,1\}} p_i \sum_{(l,m) \in \{0,1\}^2} p_{lm|i} f_R(r \mid S_1 + S_2 = a_{lm}) \\ &= \arg \max_{i \in \{0,1\}} p_i \sum_{(l,m) \in \{0,1\}^2} p_{lm|i} f_Z(r - a_{lm}), \end{aligned} \quad (1)$$

where f_R and f_Z are the probability density functions (pdfs) of the received signal R and channel noise variable Z , respectively, $p_{lm|i} \triangleq \Pr(X_1 = l, X_2 = m \mid X = i)$, and $a_{lm} \in \mathcal{C}$ denotes the superimposed constellation symbol associated with $X_1 = l$ and $X_2 = m$. In the case of a tie, we choose to detect a 0. This is an arbitrary decision because the probability of a tie is always zero since the noise is a continuous random variable. The conditional probabilities $p_{lm|i}$ can be expressed as follows in terms of the sensor crossover probabilities:

$$\begin{aligned} p_{11|0} &= p_{00|1} = \epsilon_1 \epsilon_2, \quad p_{00|0} = p_{11|1} = (1 - \epsilon_1)(1 - \epsilon_2), \\ p_{01|0} &= p_{10|1} = (1 - \epsilon_1)\epsilon_2, \quad p_{10|0} = p_{01|1} = \epsilon_1(1 - \epsilon_2). \end{aligned} \quad (2)$$

The real line is partitioned into two decision regions, \mathcal{D}_0 and $\mathcal{D}_1 = \mathcal{D}_0^c$, where $\mathcal{D}_i = \{r \in \mathbb{R} \mid \hat{x}(r) = i\}$, $i = 0, 1$.

III. SUMMARY OF MAIN RESULTS

We herein summarize our main results. Specifically, for fixed parameters p_1 , ϵ_1 , ϵ_2 , N_0 , P_1^{\max} and P_2^{\max} , we show that the optimal constellation designs for \mathcal{C}_1 and \mathcal{C}_2 which achieve the minimum error probability, P_{err}^* are expressed as $\mathcal{C}_i = \{c_{0,i}, c_{1,i}\} = \left\{ -\sqrt{\frac{p_1}{p_0} P_i^*}, \sqrt{\frac{p_0}{p_1} P_i^*} \right\}$, for $i \in \{1, 2\}$, where the optimal power allocations P_i^* are separated into three cases. The conditions for each case are given in Table I and the optimization results are summarized in Table II.

For Cases II and III in Table I, the decision boundary, x^* , is the unique root of (6) corresponding to P_1^* and P_2^* .

In Table II, we used the quantities

$$\tilde{P}_2 \triangleq \frac{N_0 p_1 p_0}{2\sqrt{P_1^{\max}}} \ln \frac{(1 - \epsilon_1 - \epsilon_2)^2 - \Lambda}{(\epsilon_2 - \epsilon_1)^2 - \Lambda}, \quad (3)$$

TABLE II
OPTIMAL POWER ALLOCATION RESULTS

Case	P_1^*	P_2^*	P_{err}^*	$\lim_{N_0 \rightarrow 0} P_{\text{err}}^*$
I	0	0	p_1	p_1
II	$\sqrt{P_1^{\max}}$	$\sqrt{P_2^{\max}}$	see (10)	see (19)
III	$\sqrt{P_1^{\max}}$	$\min(\sqrt{P_2^{\max}}, \tilde{P}_2)$	see (18)	ϵ_1

with

$$\Lambda \triangleq \frac{(p_0 - p_1)^2}{p_0 p_1} (1 - \epsilon_1)(1 - \epsilon_2)\epsilon_1 \epsilon_2.$$

Note that the expression for \tilde{P}_2 is always real valued when the conditions of Case III are met. Also note that because of the assumption $0 < \epsilon_1 \leq \epsilon_2 < 0.5$, the conditions for the three cases are numerically consistent, i.e., we have that

$$0 < \frac{\epsilon_1 \epsilon_2}{1 - \epsilon_1 - \epsilon_2 + 2\epsilon_1 \epsilon_2} < \frac{\epsilon_1 - \epsilon_1 \epsilon_2}{\epsilon_1 + \epsilon_2 - 2\epsilon_1 \epsilon_2} \leq 0.5,$$

where the last inequality holds with equality if and only if $\epsilon_1 = \epsilon_2$. These results will be further analyzed and discussed in later sections of this paper. The most interesting and counter-intuitive result is that in Case III, the optimal power allocation is not to necessarily use all of the available power for Sensor 2. The remainder of this paper is dedicated to prove these results and illustrate them via numerical examples and simulations.

IV. PROOF OF MAIN RESULTS

First, we use Theorem 1 to show that the constellation design optimization problem can be restricted to a set of asymmetric constellations, parameterized by each sensor's power allocation. Then we analyze the boundary points between the decision regions \mathcal{D}_0 and \mathcal{D}_1 (decision boundaries) using this optimal asymmetric design. The characterization of these decision boundaries splits the problem into the three cases given in Table I. For Case I, Proposition 1 shows the trivial nature of the decision boundaries, and thus also the optimization in this case. For Case II, Theorem 2 shows that using all allocated power for both sensors is optimal. Finally, in Case III, Theorem 3 gives the globally optimal power allocation for Sensor 2. Combining this result with Theorems 4 and 5, which show that the error probability decreases in both sensor powers until reaching the global minimum, yields the overall optimal power allocation under the given power constraints. The majority of the proof details for the main theorems are given in the appendices, while an overview and intuitive explanations are provided in this section.

Theorem 1: For any combination of binary constellations $\mathcal{C} = \mathcal{C}_1 + \mathcal{C}_2$, there exists a constellation pattern $\mathcal{C}^* = \mathcal{C}_1^* + \mathcal{C}_2^*$ which has equal error probability, equal or better power consumption, with the composition $\mathcal{C}_i^* = \left\{ -\sqrt{\frac{p_1}{p_0}} P_i, \sqrt{\frac{p_0}{p_1}} P_i \right\}$, for some $P_i \in \mathbb{R}$, $i \in \{1, 2\}$.

Proof: In a Gaussian MAC using MAP detection, the error probability is the same for constellations that are translations of each other. Hence, constellations with the same distances between constellation points will have the same error performance. The distances between the points in the joint constellation \mathcal{C} are determined by the distances between

the points in the individual constellations $\mathcal{C}_i = \{c_{0,i}, c_{1,i}\}$, $i \in \{1, 2\}$. Let the constellation distance, d_i be defined as follows:

$$d_i \triangleq c_{1,i} - c_{0,i}, \quad i \in \{1, 2\}. \quad (4)$$

We will minimize the average power consumption for each sensor while maintaining constellation distance d_i . This is computed below substituting in the constraint from (4):

$$P_i^2 = E[S_i^2] = p_0 c_{0,i}^2 + p_1 c_{1,i}^2 = c_{1,i}^2 - 2p_0 d_i c_{1,i} + p_0 d_i^2.$$

This is a simple quadratic function of $c_{1,i}$, which is minimized at $c_{1,i} = p_0 d_i$, $c_{0,i} = -p_1 d_i$. Substituting this back into the expression of P_i^2 , we see that the minimum power has the form $P_i^{*2} = p_1 p_0 d_i^2$. Finally, rearranging for $d_i = \frac{1}{\sqrt{p_1 p_0}} P_i^*$ shows that the minimum power constellation has the form:

$$c_{0,i} = -\sqrt{\frac{p_1}{p_0}} P_i, \quad c_{1,i} = \sqrt{\frac{p_0}{p_1}} P_i, \quad i \in \{1, 2\}. \quad \blacksquare$$

Using the result of Theorem 1, we can restrict the optimization search to constellations which take the following asymmetric form. $\mathcal{C}_i = \{c_{0,i}, c_{1,i}\} = \left\{ -\sqrt{\frac{p_1}{p_0}} P_i, \sqrt{\frac{p_0}{p_1}} P_i \right\}$, where $P_i \in [0, \sqrt{P_i^{\max}}]$ for $i \in \{1, 2\}$. To simplify notation, we define the following two symbols which represent these optimal asymmetric parameters:

$$\alpha \triangleq \sqrt{\frac{p_0}{p_1}}, \quad \beta \triangleq \sqrt{\frac{p_1}{p_0}}. \quad (5)$$

The relationship $\alpha + \beta = \frac{1}{\sqrt{p_0 p_1}}$ will be used often in the remaining analysis. The problem has now been reduced to finding the optimal power allocations, P_1 and P_2 .

A. Decision Boundaries

To analyze the error probabilities, we first must understand the behaviour of the decision regions \mathcal{D}_0 and \mathcal{D}_1 . To characterize these regions, we take the difference between the two terms in (1) and manipulate the expressions to give

$$\begin{aligned} & \Pr(X = 1 | R = r) - \Pr(X = 0 | R = r) \\ &= \sum_{(l,m) \in \{0,1\}^2} (p_1 p_{lm|1} - p_0 p_{lm|0}) f_Z(r - a_{lm}) \\ &= \frac{1}{\sigma \sqrt{2\pi}} \sum_{(l,m) \in \{0,1\}^2} (p_1 p_{lm|1} - p_0 p_{lm|0}) e^{-\frac{(r - a_{lm})^2}{N_0}}. \end{aligned}$$

We are interested in the sign of this expression, so we simplify using the following forms of the restricted constellation points:

$$\begin{aligned} a_{11} &= \alpha(P_1 + P_2), & a_{01} &= -\beta P_1 + \alpha P_2, \\ a_{10} &= \alpha P_1 - \beta P_2, & a_{00} &= -\beta(P_1 + P_2), \end{aligned}$$

which gives the following function of x , which has the same sign as the original expression for any fixed P_1 and P_2 :

$$w(x) = a e^{\frac{2(\alpha+\beta)(P_1+P_2)x}{N_0}} + b e^{\frac{2(\alpha+\beta)P_1 x}{N_0}} + c e^{\frac{2(\alpha+\beta)P_2 x}{N_0}} + d, \quad (6)$$

where

$$\begin{aligned} a &\triangleq \bar{a}e^{-\frac{\alpha^2(P_1+P_2)^2}{N_0}}, & b &\triangleq \bar{b}e^{-\frac{(\alpha P_1 - \beta P_2)^2}{N_0}}, \\ c &\triangleq \bar{c}e^{-\frac{(\beta P_1 - \alpha P_2)^2}{N_0}}, & d &\triangleq \bar{d}e^{-\frac{\beta^2(P_1+P_2)^2}{N_0}}, \end{aligned}$$

and

$$\begin{aligned} \bar{a} &\triangleq p_1 p_{11|1} - p_0 p_{11|0}, & \bar{b} &\triangleq p_1 p_{10|1} - p_0 p_{10|0}, \\ \bar{c} &\triangleq p_1 p_{01|1} - p_0 p_{01|0}, & \bar{d} &\triangleq p_1 p_{00|1} - p_0 p_{00|0}. \end{aligned} \quad (7)$$

Using (6), we can characterize the decision regions as $\mathcal{D}_0 = \{x \in \mathbb{R} \mid w(x) \leq 0\} = \mathcal{D}_1^c$. Note that by the assumptions on p_1 , ϵ_1 and ϵ_2 , we have that $\bar{d} < 0$, which implies that $w(x)$ is negative as $x \rightarrow -\infty$ for any P_1 and P_2 (hence the MAP rule detects a 0). Thus, we can completely determine these regions by the boundary points between \mathcal{D}_0 and \mathcal{D}_1 . These boundary points are the same as where $w(x)$ crosses from negative to positive, or vice-versa. Thus, it is relevant to analyze the set $\mathcal{X} = \{x \in \mathbb{R} \mid w(x) = 0\}$. Note that applying the results of [21, Corollary 3.2], we know that the size of this set is restricted to $|\mathcal{X}| \in \{0, 1, 2, 3\}$. Unfortunately, there is not a general way to solve for the values $x \in \mathcal{X}$ analytically. However, the problem can be split into three cases which can be analyzed without knowing these values explicitly. The decision regions can be expressed as unions of intervals using these boundary points. For example, if $\mathcal{X} = \{x\}$, then $\mathcal{D}_0 = (-\infty, x]$, whereas if $\mathcal{X} = \{x_1, x_2, x_3\}$, with $x_1 < x_2 < x_3$ then $\mathcal{D}_0 = (-\infty, x_1] \cup [x_2, x_3]$.

B. Case I: $0 \leq p_1 \leq \frac{\epsilon_1 \epsilon_2}{1 - \epsilon_1 - \epsilon_2 + 2\epsilon_1 \epsilon_2}$

To analyze the error probability, we must first understand how the decision regions behave. Using the defining relationships of Case I, we obtain the following result.

Proposition 1: In Case I, there are no real solutions to the equation $w(x) = 0$, where $w(x)$ is given in (6).

Proof: Each of the following inequalities hold due to the condition of Case I, and $p_1 \leq 0.5$, $0 < \epsilon_1 \leq \epsilon_2 < 0.5$:

$$\begin{aligned} \bar{a} &= p_1 p_{11|1} - p_0 p_{11|0} \\ &= (1 - \epsilon_1 - \epsilon_2 + 2\epsilon_1 \epsilon_2) \left(p_1 - \frac{\epsilon_1 \epsilon_2}{1 - \epsilon_1 - \epsilon_2 + 2\epsilon_1 \epsilon_2} \right) \\ &\leq 0 \implies a \leq 0, \end{aligned}$$

$$\begin{aligned} \bar{b} &= p_1 p_{10|1} - p_0 p_{10|0} \\ &= (\epsilon_1 + \epsilon_2 - 2\epsilon_1 \epsilon_2) \left(p_1 - \frac{\epsilon_1 - \epsilon_1 \epsilon_2}{\epsilon_1 + \epsilon_2 - 2\epsilon_1 \epsilon_2} \right) < 0 \\ \implies b &< 0, \end{aligned}$$

$$\begin{aligned} \bar{c} &= p_1 p_{01|1} - p_0 p_{01|0} \\ &= (\epsilon_1 + \epsilon_2 - 2\epsilon_1 \epsilon_2) \left(p_1 - \frac{\epsilon_2 - \epsilon_1 \epsilon_2}{\epsilon_1 + \epsilon_2 - 2\epsilon_1 \epsilon_2} \right) < 0 \\ \implies c &< 0, \end{aligned}$$

$$\begin{aligned} \bar{d} &= p_1 p_{00|1} - p_0 p_{00|0} \\ &= (1 - \epsilon_1 - \epsilon_2 + 2\epsilon_1 \epsilon_2) \left(p_1 - \frac{1 - \epsilon_1 - \epsilon_2 + \epsilon_1 \epsilon_2}{1 - \epsilon_1 - \epsilon_2 + 2\epsilon_1 \epsilon_2} \right) \\ &< 0 \implies d < 0. \end{aligned}$$

Thus $w(x) < 0 \forall x \in \mathbb{R}$ and $w(x)$ has no real roots. ■

Since there are no roots of (6), there are also no decision boundaries in Case I. Thus, no matter what the received signal is, the optimal detection will always be $\hat{x} = 0$ (i.e., $\mathcal{D}_0 = \mathbb{R}$). Hence, the error probability is only dependent on the source probability p_1 . In this case, the sensors are not able to send any useful data, so they should not send anything at all. We conclude that the optimal power allocation and corresponding error performance are expressed as follows:

$$P_1^{\text{Case I}} = 0, \quad P_2^{\text{Case I}} = 0, \quad P_{\text{err}}^{\text{Case I}} = p_1.$$

C. Case II: $\frac{\epsilon_1 \epsilon_2}{1 - \epsilon_1 - \epsilon_2 + 2\epsilon_1 \epsilon_2} < p_1 \leq \frac{\epsilon_1 - \epsilon_1 \epsilon_2}{\epsilon_1 + \epsilon_2 - 2\epsilon_1 \epsilon_2}$

Using a similar approach as in the proof of Proposition 1, we can show the following properties about the coefficients of (6) in this case:

$$a > 0, \quad b \leq 0, \quad c \leq 0, \quad d < 0.$$

We can now characterize the decision regions as follows.

Proposition 2: In Case II, there is exactly one real root to $w(x)$ in (6) for any $P_1, P_2 > 0$. Further, this root is also a decision boundary between \mathcal{D}_0 and \mathcal{D}_1 .

Proof: Let $P_1, P_2 > 0$. First we show that there exists at least one real solution to $w(x) = 0$. We use the fact that $w(x)$ is continuous and that its asymptotic behaviours are:

$$\lim_{x \rightarrow -\infty} w(x) = d, \quad \lim_{x \rightarrow \infty} w(x) = \infty.$$

Since $d < 0$ and $w(x)$ is continuous, it must have at least one root. Next we show that $w(x)$ can have at most one root by showing that once it becomes non-negative, the derivative is always strictly positive, so it can never have another zero. Assume $w(x) \geq 0$, we then have:

$$\begin{aligned} \frac{dw}{dx} &= \frac{2(\alpha + \beta)}{N_0} \left((P_1 + P_2) a e^{\frac{2(\alpha + \beta)(P_1 + P_2)x}{N_0}} \right. \\ &\quad \left. + P_1 b e^{\frac{2(\alpha + \beta)P_1 x}{N_0}} + P_2 c e^{\frac{2(\alpha + \beta)P_2 x}{N_0}} \right) \\ &= \frac{2(\alpha + \beta)}{N_0} \left((P_1 + P_2) w(x) - P_2 b e^{\frac{2(\alpha + \beta)P_1 x}{N_0}} \right. \\ &\quad \left. - P_1 c e^{\frac{2(\alpha + \beta)P_2 x}{N_0}} - (P_1 + P_2) d \right) > 0. \end{aligned}$$

This shows that $w(x)$ has exactly one real root, and this root is a boundary point between \mathcal{D}_0 and \mathcal{D}_1 as desired. ■

Since there is a unique decision boundary, the decision regions will have the form $\mathcal{D}_0 = (-\infty, x]$, where x is the root of (6) corresponding to P_1 and P_2 . We can express the error probability at any $P_1, P_2 > 0$ using the following expression:

$$\begin{aligned} P_{\text{err}}(P_1, P_2) &= \sum_{(l,m) \in \{0,1\}^2} (p_1 p_{lm|1} - p_0 p_{lm|0}) Q \left(\frac{a_{lm} - x}{\sigma} \right) \\ &\quad + p_0 p_{lm|0}, \end{aligned} \quad (8)$$

where Q is the Gaussian tail distribution function, defined as

$$Q(x) = \frac{1}{\sqrt{2\pi}} \int_x^\infty e^{-\frac{u^2}{2}} du,$$

a_{lm} are the constellation points and x is the root of (6) corresponding to P_1 and P_2 . We also give the following upper bound on the error probability.

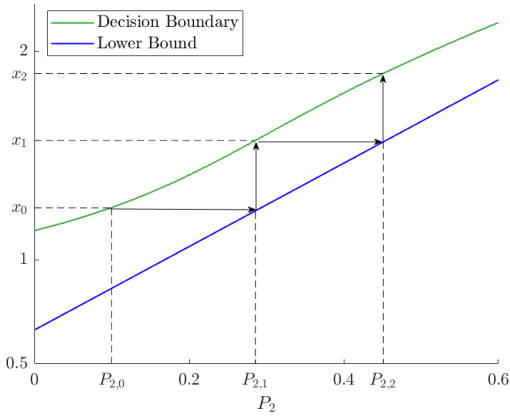


Fig. 1. Graphical representation of the sequence $\{P_{2,i}\}_{i=0}^{\infty}$ and corresponding decision boundaries $\{x_i\}_{i=0}^{\infty}$.

Proposition 3: If $P_1, P_2 > 0$ and x is the corresponding unique decision boundary, then for any $\hat{x} \in \mathbb{R}$, the following is an upper bound on the error probability

$$P_{\text{err},\hat{x}}^{\text{UB}}(P_1, P_2) \triangleq \sum_{(l,m) \in \{0,1\}^2} (p_1 p_{l_m|1} - p_0 p_{l_m|0}) Q\left(\frac{a_{lm} - \hat{x}}{\sigma}\right) + p_0 p_{l_m|0}. \quad (9)$$

Proof: This expression corresponds to the error probability associated to using a decision boundary \hat{x} . Since the true decision boundary, x , from the MAP detection rule is optimal, this must be an upper bound. ■

This upper bound is used to show the following main result about the error probability as a function of P_1 and P_2 .

Theorem 2: In Case II, $P_{\text{err}}(P_1, P_2)$ is decreasing in P_1 and P_2 for $P_1, P_2 > 0$.

Proof: See Appendix A. ■

While the detailed proof of this theorem is provided in Appendix A, we herein highlight its main steps. For either of the sensors (say, Sensor 2) we first establish a lower bound on the value of the decision boundary for any value of P_2 . For some fixed $P_{2,0}$, we use this lower bound to define a step-wise increasing sequence $\{P_{2,i}\}_{i=0}^{\infty}$, as illustrated in Fig. 1.

Although the error expression as given in (8) cannot be analytically minimized because of the dependence on the decision boundary, x , the upper bound given in (9) can be analyzed for any fixed \hat{x} . We show by direct derivative analysis that for any adjacent terms in the sequence, $P_{2,i}$ and $P_{2,i+1}$, there is an upper bound with equality at $P_{2,i}$ and is decreasing until $P_{2,i+1}$. This shows that the error probability decreases from $P_{2,i}$ to $P_{2,i+1}$, as illustrated in Fig. 2.

Using the results of Theorem 2, we conclude that the optimal power allocation and corresponding error performance can be expressed as follows, where $p_{l_m|i}$ are as given in (2), x^* is the root to (6) and a_{lm}^* are the constellation points corresponding to P_1^* and P_2^* .

$$P_1^{\text{Case II}} = \sqrt{P_1^{\text{max}}}, \quad P_2^{\text{Case II}} = \sqrt{P_2^{\text{max}}},$$

$$P_{\text{err}}^{\text{Case II}} = \sum_{(l,m) \in \{0,1\}^2} (p_1 p_{l_m|1} - p_0 p_{l_m|0}) Q\left(\frac{a_{lm}^* - x^*}{\sigma}\right) + p_0 p_{l_m|0}. \quad (10)$$

The corresponding optimal decision region is $\mathcal{D}_0 = (-\infty, x^*]$.

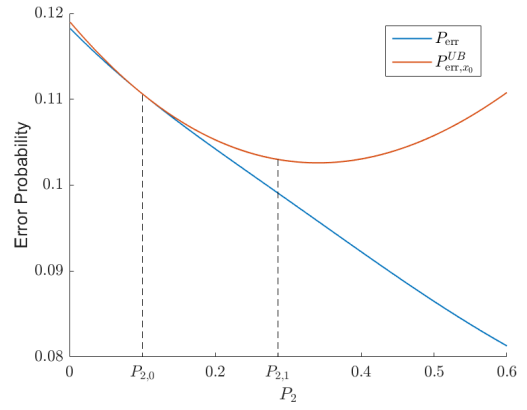


Fig. 2. A depiction of the error probability decreasing between consecutive terms of the sequence $\{P_{2,i}\}_{i=0}^{\infty}$.

D. Case III: $\frac{\epsilon_1 - \epsilon_1 \epsilon_2}{\epsilon_1 + \epsilon_2 - 2\epsilon_1 \epsilon_2} < p_I \leq 0.5$

First note that the condition of this case implies $\epsilon_1 \neq \epsilon_2$. Also using the same reasoning as in the proof of Proposition 1, we make the following observations about the coefficients of $w(x)$ in (6):

$$a > 0, \quad b > 0, \quad c < 0, \quad d < 0.$$

We define the following functions of P_1 , where \bar{a} , \bar{b} , \bar{c} and \bar{d} are as defined in (7):

$$\tilde{P}_2(P_1) \triangleq \frac{N_0}{2(\alpha + \beta)^2 P_1} \ln \frac{\bar{a}\bar{d}}{\bar{b}\bar{c}}, \quad (11)$$

$$K_\alpha(P_1) \triangleq \frac{N_0}{2(\alpha + \beta) P_1} \ln \frac{\bar{a}}{-\bar{c}} - \frac{\alpha - \beta}{2} P_1, \quad (12)$$

$$K_\beta(P_1) \triangleq \frac{N_0}{2(\alpha + \beta) P_1} \ln \frac{-\bar{d}}{\bar{b}} + \frac{\alpha - \beta}{2} P_1. \quad (13)$$

The condition for Case III combined with the other assumptions on the problem's parameters ensure that these functions are real valued for all $P_1 > 0$. Also note that expanding (11) at $P_1 = \sqrt{P_1^{\text{max}}}$ gives the expression in (3). We begin with the following result which is used numerous times over the analysis of this case.

Proposition 4: For any $P_1, P_2 > 0$ the following two statements are true:

$$x \lesseqgtr \alpha P_2 - K_\alpha(P_1) \implies a e^{\frac{2(\alpha + \beta) P_1 x}{N_0}} + c \lesseqgtr 0, \quad (14)$$

$$x \lesseqgtr -\beta P_2 + K_\beta(P_1) \implies b e^{\frac{2(\alpha + \beta) P_1 x}{N_0}} + d \lesseqgtr 0, \quad (15)$$

where the symbol \lesseqgtr means that the statements hold for any of the relations $<$, $>$ or $=$, consistently in the each line.

Proof: These statements follow directly from rearranging these equations and using the definitions of K_α and K_β in (12) and (13), respectively. The steps are the same as in the proof of Proposition 7. ■

This result is used for many of the remaining proofs in this section. For instance, a direct application of these statements gives the following bounds on the roots of (6).

Proposition 5: In Case III, for any $P_1, P_2 > 0$, if x is a corresponding root of (6), then it must satisfy

$$\begin{cases} x \in (\alpha P_2 - K_\alpha(P_1), -\beta P_2 + K_\beta(P_1)), & P_2 < \tilde{P}_2(P_1) \\ x = \alpha P_2 - K_\alpha(P_1) = -\beta P_2 + K_\beta(P_1), & P_2 = \tilde{P}_2(P_1) \\ x \in (-\beta P_2 + K_\beta(P_1), \alpha P_2 - K_\alpha(P_1)), & P_2 > \tilde{P}_2(P_1) \end{cases} \quad (16)$$

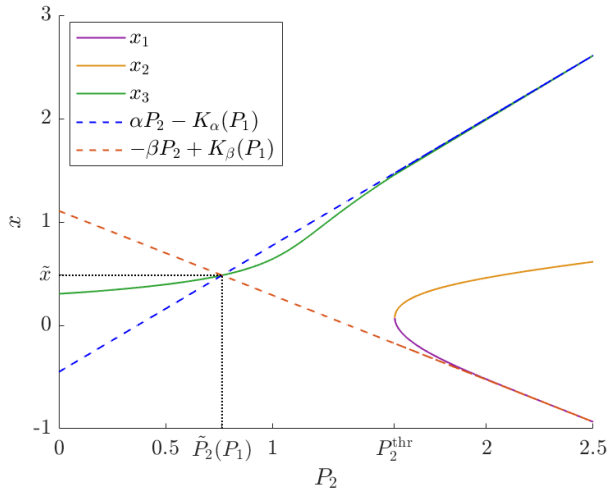


Fig. 3. The roots of (6), x_1 , x_2 and x_3 , as a function of P_2 in Case III ($p_1 = 0.4$, $\epsilon_1 = 0.01$, $\epsilon_2 = 0.05$, $N_0 = 1$, $P_1 = 1$). The decision regions can be read as: for $P_2 < P_2^{\text{thr}} \approx 1.6$, $\mathcal{D}_0 = (-\infty, x_3]$. Otherwise, $\mathcal{D}_0 = (-\infty, x_1] \cup [x_2, x_3]$.

Proof: First we note that these intervals are valid and have non-zero length since

$$\begin{aligned} & -\beta P_2 + K_\beta(P_1) - (\alpha P_2 - K_\alpha(P_1)) \\ & = K_\alpha(P_1) + K_\beta(P_1) - (\alpha + \beta)P_2 \\ & = (\alpha + \beta)(\tilde{P}_2(P_1) - P_2), \end{aligned}$$

so

$$P_2 \leq \tilde{P}_2(P_1) \implies \alpha P_2 - K_\alpha(P_1) \leq -\beta P_2 + K_\beta(P_1).$$

If x is outside these intervals, then we apply (14) and (15) from Proposition 4 to see that $w(x) \neq 0$, so x could not be a root of (6). ■

For a fixed $P_1 > 0$, the bounds described in Proposition 5 form two lines with respect to P_2 which intersect at $\tilde{P}_2(P_1)$. An illustration of these bounds can be seen in Fig. 3.

This is another useful result which is referred to multiple times in the remaining proofs in this section. For example, Propositions 4 and 5 are used to prove the following result about the number of decision boundaries.

Proposition 6: In Case III, for any $P_1, P_2 > 0$, there will be one or three boundary points between \mathcal{D}_0 and \mathcal{D}_1 . Further, if $P_2 \in (0, \tilde{P}_2(P_1)]$ there is exactly one boundary point between \mathcal{D}_0 and \mathcal{D}_1 .

Proof: Let $P_1, P_2 > 0$. We have the following asymptotic behaviours of $w(x)$ in (6):

$$\lim_{x \rightarrow -\infty} w(x) = d, \quad \lim_{x \rightarrow \infty} w(x) = \infty.$$

Since $d < 0$, and w is continuous, we conclude that there must be an odd number of crossing points. Combining this fact with [21, Corollary 3.2] yields that there will be one or three crossing points. Now let $P_2 \in (0, \tilde{P}_2(P_1)]$. We assume $w(x) = 0$, then performing the same derivative analysis as in the proof of Proposition 2 yields:

$$\begin{aligned} \frac{dw}{dx} = & \frac{-2(\alpha + \beta)}{N_0} \left(P_2 \left(b e^{\frac{2(\alpha + \beta)P_1 x}{N_0}} + d \right) \right. \\ & \left. + P_1 \left(c e^{\frac{2(\alpha + \beta)P_2 x}{N_0}} + d \right) \right) > 0. \end{aligned}$$

This last inequality is true since Propositions 4 and 5 imply

$$b e^{\frac{2(\alpha + \beta)P_1 x}{N_0}} + d \leq 0.$$

Therefore $w(x)$ is strictly increasing at any zero, and hence must only have one root, and this root must be a boundary point between \mathcal{D}_0 and \mathcal{D}_1 as desired. ■

We do not provide the exact condition for when there are three decision boundaries because it is not necessary for the remaining optimization, and would require explicit analysis of the roots of (6), which is not clearly possible. The typical behaviour is that for fixed P_1 , there will be one decision boundary for all P_2 less than some threshold value, and three decision boundaries for all values larger than this threshold. These results are also demonstrated in Fig. 3.

Using Proposition 6, we conclude that the error probability in Case III can have two possible expressions based on the number of decision boundaries. If there is a single decision boundary, x , then the error expression will have the same form as in (8). If there are three decision boundaries, $x_1 < x_2 < x_3$, then the error expression has the following form:

$$\begin{aligned} P_{\text{err}}(P_1, P_2) & = \sum_{(l,m) \in \{0,1\}^2} (p_1 p_{l|m|1} - p_0 p_{l|m|0}) \left(Q \left(\frac{a_{lm} - x_1}{\sigma} \right) \right. \\ & \quad \left. - Q \left(\frac{a_{lm} - x_2}{\sigma} \right) + Q \left(\frac{a_{lm} - x_3}{\sigma} \right) \right) + p_0 p_{l|m|0}. \quad (17) \end{aligned}$$

These expressions for error probability are used to show the following theorems for optimizing error probability in Case III.

Theorem 3: In Case III, $P_{\text{err}}(P_1, \tilde{P}_2(P_1)) < P_{\text{err}}(P_1, P_2)$, $\forall P_1 > 0, P_2 \neq \tilde{P}_2(P_1)$.

Proof: See Appendix B. ■

This gives an analytic expression for the global minimizer of the error probability with respect to P_2 . The main intuition behind this result relies on splitting the error function into two simpler parts, which are shown to be minimized along the same linear bounds in Fig. 3. Since the two lines intersect at $\tilde{P}_2(P_1)$, both parts of the error function are minimized, hence the entire error function is also minimized.

Although we have found a global minimum with respect to P_2 , it is still necessary to determine the optimal constellation when there is not enough power to use the global minimum, i.e., if $\sqrt{P_2^{\text{max}}} < \tilde{P}_2(P_1)$. The following theorem provides a sufficient result for this situation.

Theorem 4: In Case III, if $0 < P_1, 0 < P_2 < P_2' < \tilde{P}_2(P_1)$, then $P_{\text{err}}(P_1, P_2) > P_{\text{err}}(P_1, P_2')$.

Proof: See Appendix C. ■

The technical details are slightly more complicated, but the reasoning behind this proof is very similar to that of Theorem 2. The same sequentially decreasing idea is applied, except more care is taken to address both bounding lines in Case III, as opposed to the single bounding line in Case II.

Combining Theorems 3 and 4 we can conclude that in Case III, the optimal power allocation for P_2 given $P_1 > 0$ is

$$P_2^*(P_1) = \min(\sqrt{P_2^{\text{max}}}, \tilde{P}_2(P_1)).$$

Now that we have the optimal P_2 allocation for a fixed P_1 , we can analyze the P_1 optimization using this result.

Theorem 5: In Case III, $P_{\text{er}}(P_1, P_2^*(P_1))$ is decreasing in P_1 , for all $P_1 > 0$.

Proof: See Appendix D. ■

The proof of this result is mainly a direct derivative analysis using the closed form expression for $\tilde{P}_2(P_1)$ and the corresponding decision boundary, \hat{x} . The implication of this result is that the less noisy sensor should use all available power. Further, we note $\tilde{P}_2(P_1)$ is decreasing in P_1 . This results in the generally intuitive behaviour to allocate more power to the more reliable sensor, and less to the worse sensor.

Combining the results of Theorems 3, 4 and 5 implies that the optimal power allocation and corresponding error performance can be expressed as follows, where x^* is the root of (6), and a_{lm}^* are the corresponding constellation points to P_1^* and P_2^* :

$$\begin{aligned} P_1^{\text{Case III}} &= \sqrt{P_1^{\text{max}}}, \\ P_2^{\text{Case III}} &= \min(\sqrt{P_2^{\text{max}}}, \tilde{P}_2(\sqrt{P_1^{\text{max}}}), \\ P_{\text{er}}^{\text{Case III}} &= \sum_{(l,m) \in \{0,1\}^2} (p_1 p_{lm|1} - p_0 p_{lm|0}) Q\left(\frac{a_{lm}^* - x^*}{\sigma}\right) + p_0 p_{1m|0}. \end{aligned} \quad (18)$$

The corresponding optimal decision region is $\mathcal{D}_0 = (-\infty, x^*]$. If $P_2^* = \tilde{P}_2(\sqrt{P_1^{\text{max}}}) = \tilde{P}_2$ as in (3), then the optimal decision boundary has the explicit form $x^* = \alpha \tilde{P}_2 - K_\alpha(\sqrt{P_1^{\text{max}}})$.

E. High SNR Behaviour

For this analysis it is defined that high SNR means $N_0 \rightarrow 0$. This is a reasonable assumption since each sensor's SNR should be growing at similar rates, and one sensor should not have infinitely more power than the other. In Case I, there is nothing to consider, since the error probability is constant. In Cases II and III, the high SNR behaviour can be analyzed by considering a system that knows which point in the constellation \mathcal{C} was sent. Note this is equivalent to knowing X_1 and X_2 perfectly, except if two constellation points overlap, i.e., $a_{ij} = a_{i'j'}$ for some $i \neq i', j \neq j'$. Also note that the high SNR behaviour of only sending Sensor i is always ϵ_i , $i \in \{1, 2\}$. In the case that both sensor values are used, the following is the MAP detection rule for knowing $X_1 = x_1$ and $X_2 = x_2$:

$$\begin{aligned} \hat{x}(x_1, x_2) &= \arg \max_{i \in \{0,1\}} \Pr(X = i \mid X_1 = x_1, X_2 = x_2) \\ &= \arg \max_{i \in \{0,1\}} p_i p_{x_1 x_2 | i}. \end{aligned}$$

The decision conditions can be expressed in terms of the constants defined in (6) as follows:

$$\begin{aligned} \bar{a} > 0 &\iff \hat{x}(1, 1) = 1, & \bar{b} > 0 &\iff \hat{x}(1, 0) = 1, \\ \bar{c} > 0 &\iff \hat{x}(0, 1) = 1, & \bar{d} > 0 &\iff \hat{x}(0, 0) = 1. \end{aligned}$$

1) *Case II:* Based on the values of $\bar{a}, \bar{b}, \bar{c}, \bar{d}$ in this case, we have the following detection rule:

$$\begin{aligned} \hat{x}(1, 1) &= 1, & \hat{x}(1, 0) &= 0, \\ \hat{x}(0, 1) &= 0, & \hat{x}(0, 0) &= 0. \end{aligned}$$

Since $\hat{x}(1, 0) = \hat{x}(0, 1)$, it does not matter if these two constellation points overlap (and these are the only two constellation points which can possibly overlap). Finally, the high SNR behaviour is calculated to be

$$\begin{aligned} \lim_{N_0 \rightarrow 0} P_{\text{er}}^*(P_1^*, P_2^*) &= p_1(p_{00|1} + p_{01|1} + p_{10|1}) + p_0 p_{11|0} \\ &= \epsilon_1 \epsilon_2 + p_1(\epsilon_1 + \epsilon_2 - 2\epsilon_1 \epsilon_2). \end{aligned} \quad (19)$$

2) *Case III:* In this case, there are two interesting cases to consider. First, for the optimal allocation $P_2 = P_2^*$, we have that $P_2^* \rightarrow 0$ for high SNR; so the error performance in this case approaches the performance of only sending Sensor 1, which is ϵ_1 . In the alternative case that both sensors use all their power, the detection rule is as follows:

$$\begin{aligned} \hat{x}(1, 1) &= 1, & \hat{x}(1, 0) &= 1, \\ \hat{x}(0, 1) &= 0, & \hat{x}(0, 0) &= 0. \end{aligned}$$

If no constellation points overlap, $\hat{X} = X_1$, which implies

$$\lim_{N_0 \rightarrow 0} P_{\text{er}}(\sqrt{P_1^{\text{max}}}, \sqrt{P_2^{\text{max}}}) = \epsilon_1, \quad P_1^{\text{max}} \neq P_2^{\text{max}}.$$

However, if $P_1^{\text{max}} = P_2^{\text{max}} = P^{\text{max}}$ for some $P^{\text{max}} > 0$, then $a_{01} = a_{10}$. Let P_{er}^i , $i \in \{0, 1\}$ be the error probability if we decide to detect i for 10/01. Since $p_1 \leq p_0$ and

$$\begin{aligned} P_{\text{er}}^0 &= \epsilon_1 \epsilon_2 + p_1(\epsilon_1 + \epsilon_2 - 2\epsilon_1 \epsilon_2) \\ P_{\text{er}}^1 &= \epsilon_1 \epsilon_2 + p_0(\epsilon_1 + \epsilon_2 - 2\epsilon_1 \epsilon_2) \\ \implies P_{\text{er}}^0 &\leq P_{\text{er}}^1, \end{aligned}$$

we conclude to decide 0, and the final expression for the high SNR behaviour is

$$\lim_{N_0 \rightarrow 0} P_{\text{er}}(\sqrt{P^{\text{max}}}, \sqrt{P^{\text{max}}}) = \epsilon_1 \epsilon_2 + p_1(\epsilon_1 + \epsilon_2 - 2\epsilon_1 \epsilon_2).$$

These results are demonstrated in Fig. 11, where the curve for using both sensors at their max power has a larger end behaviour than the derived optimal constellation design. Note that in Case II, $P_{\text{er}}^0 < \epsilon_1$, but in Case III, $\epsilon_1 < P_{\text{er}}^0 < \epsilon_2$.

V. NUMERICAL AND SIMULATION RESULTS

In this section, we illustrate the results of this paper numerically for specific parameter sets of the problem setup. We show that the theoretical results proven in the previous section are also supported by simulated experiments. In what follows, the SNR is defined as the geometric average of the available power allocations, reported in dB (i.e., $\text{SNR (dB)} = 10 \log_{10}(\text{SNR})$):

$$\text{SNR}^{\text{max}} \triangleq \frac{\sqrt{P_1^{\text{max}} P_2^{\text{max}}}}{N_0}. \quad (20)$$

Even though Sensor 2 does not necessarily use all of its allocated power, defining the SNR this way is sensible because the sensors have independent power constraints. If the sensors had a joint power constraint, it would be more appropriate to use the true SNR.

A. Simulated Validation of Main Results

The experimental data is produced by sending 500,000 independent source bits via two simulated sensors and MAC,

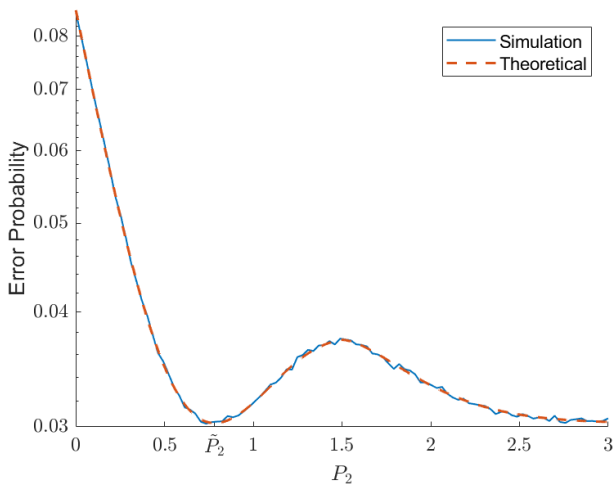


Fig. 4. Theoretical and simulated error probability in Case III ($p_1 = 0.45, \epsilon_1 = 0.01, \epsilon_2 = 0.05, P_1 = 1, N_0 = 1$).

then using the MAP detection rule given in (1), the error probability is calculated. We will show in two ways that the simulations overlap with the theoretical results. First we show that the minimization problem is solved at the correct value of P_2 in Case III. Then we show that the error probability when using the derived optimal constellation design overlaps with the simulation results at any SNR in Case II. We always use the optimal asymmetric constellation designs for these simulations, $\mathcal{C}_i = \{c_{0,i}, c_{1,i}\} = \{-\beta P_i, \alpha P_i\}$ for $i \in \{1, 2\}$. To calculate the theoretical error probability, the decision boundaries are calculated by numerically solving for the roots of (6). Then, these values are used to calculate the appropriate error expression, (8) or (17), based on the number of roots.

The error probability as a function of P_2 and SNR are shown in Figs. 4 and 5, respectively. These plots show that the simulated and theoretical error performance overlaps very well, while also noting that the simulated minimum power allocation for P_2 coincides with the theoretical results.

B. Simulated Comparison to Orthogonal Signaling

In this section, we compare the error probability of the MAC signaling system derived in this paper to an alternative signaling method of using independent (orthogonal) channels for the sensors. To set up the orthogonal signaling, it is assumed that the sensor network would have access to two independent zero-mean Gaussian communication channels with variance $\frac{N_0}{2}$. Note that we define the SNR in the orthogonal case to be the same as in (20). Even though there is more total noise when considering both orthogonal channels, this is a realistic comparison. If a system has access to two orthogonal channels with the same noise power, it can choose to only use one of the channels, which is exactly the equivalent MAC we are comparing to. We use two variations of orthogonal constellations as baseline comparisons. First, we use a simple symmetric binary phase-shift keying (BPSK) constellation design (i.e., $\mathcal{C}_i = \{c_{0,i}, c_{1,i}\} = \{-\sqrt{P_i^{\max}}, \sqrt{P_i^{\max}}\}$ for $i \in \{1, 2\}$). We also use the results of [12] which give an optimal orthogonal constellation design to be asymmetric BPSK with $\mathcal{C}_i = \{c_{0,i}, c_{1,i}\} = \{-\beta\sqrt{P_i^{\max}}, \alpha\sqrt{P_i^{\max}}\}$ for $i \in \{1, 2\}$, with α and β as defined in (5). To detect the

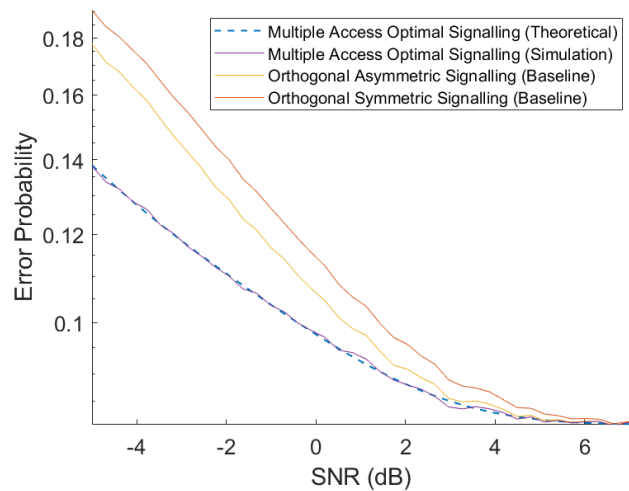


Fig. 5. Error probability as a function of SNR in Case II ($p_1 = 0.3, \epsilon_1 = 0.1, \epsilon_2 = 0.15, P_1^{\max} = 1, P_2^{\max} = 1$).

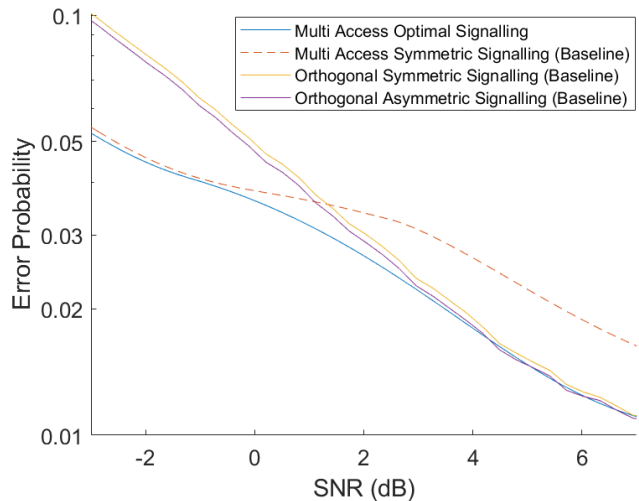


Fig. 6. Error probability as a function of SNR in Case III ($p_1 = 0.4, \epsilon_1 = 0.01, \epsilon_2 = 0.05, P_1^{\max} = 1, P_2^{\max} = 2$).

source, the receiver uses the MAP detection rule which is the two dimensional extension of (1). Since we have not analyzed the orthogonal channels case theoretically, we rely on simulation results to draw conclusions. In Figs. 5 and 6, the error probabilities are compared under two parameter sets, to show Cases II and III, respectively. Each data point is generated from 500,000 independent simulated source bits being sent through the channel. Fig. 6 also includes the error probabilities associated with using the maximum power symmetric constellation design over the MAC.

From these graphs we can see that in both Cases II and III, the derived optimal MAC constellation has better error performance than orthogonal signaling. However, in Case III (Fig. 6), orthogonal signaling can perform better than the sub-optimal multiple access symmetric constellation design. These results demonstrate that using a MAC optimally can have increased performance, while using less power and bandwidth. In Fig. 5, the maximum SNR gain of the derived optimal constellation compared to the next best option is about 2.4 dB. In Fig. 6, the maximum SNR gain is approximately 0.97 dB, occurring around 0.036 error probability.

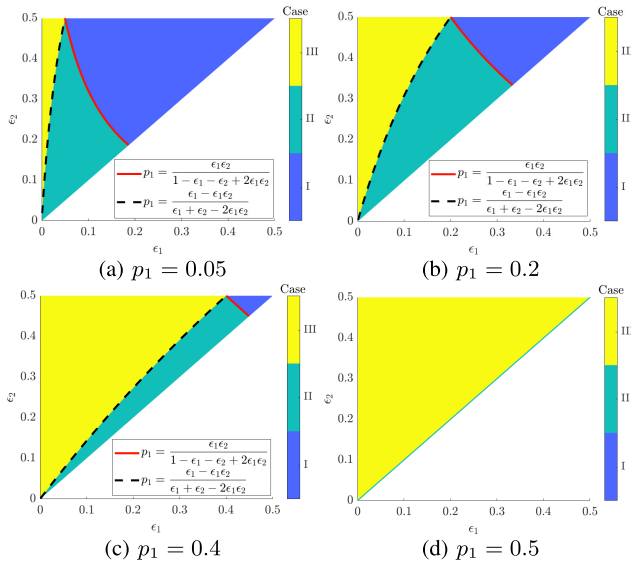


Fig. 7. Case type regions for different values of p_1 .

C. Analysis of Cases Based on Parameters p_1, ϵ_1 and ϵ_2

We analyze the behaviour of Cases I-III as a function of the parameters ϵ_1, ϵ_2 and p_1 . By fixing p_1 , we illustrate the case type regions as a colour map of ϵ_1 and ϵ_2 . Examples of these graphs are shown in Fig. 7.

We make the following observations from these diagrams. Case I occurs at large ϵ_1 and ϵ_2 values, while Case III is characterized by small ϵ_1 and large ϵ_2 . The boundaries between these regions are given exactly by the threshold equations given in Table I. As p_1 increases, the Case I region becomes smaller, while Case III becomes larger. Finally, at $p_1 = 0.5$, Case I disappears entirely, and Case II is equivalent to $\epsilon_1 = \epsilon_2$. This can intuitively be explained by noting that for any $p_1 < 0.5$, as $\epsilon_1, \epsilon_2 \rightarrow 0.5$, X_1 and X_2 become uniformly distributed and independent from the source X . This effectively removes the source information, making it useless to send over the channel (Case I). However, if $p_1 = 0.5$, X_1 and X_2 are uniformly distributed for any ϵ_1 and ϵ_2 , so there is no statistical redundancy in the source (as it is unbiased) that can be lost when observed by the sensors. Hence it is always beneficial to send the signals, which explains why Case I disappears at $p_1 = 0.5$.

D. Error Performance Vs. (P_1, P_2) and (ϵ_1, ϵ_2)

For the following examples, the constellations are parameterized by the optimal asymmetric design, $\mathcal{C}_i = \{c_{0,i}, c_{1,i}\} = \{-\beta P_i, \alpha P_i\}$, $i \in 1, 2$. Figs. 8 and 9 show the error probability as a function of P_1 and P_2 in Cases II and III, respectively.

In Fig. 8, increasing P_1 and P_2 always decreases the error probability, which reinforces the derived optimal power allocation to use all available power. Fig. 9 illustrates the following properties of Case III. First, we can see that for any fixed P_1 (vertical slice of the graph), the minimum occurs at $P_2 = \tilde{P}_2(P_1)$, the red curve. Further, moving upward from $P_2 = 0$ to $P_2 = \tilde{P}_2(P_1)$, we also see that the error probability decreases in P_2 . Finally, we can see that moving rightward along the optimal power allocation curve, $\tilde{P}_2(P_1)$, the optimal

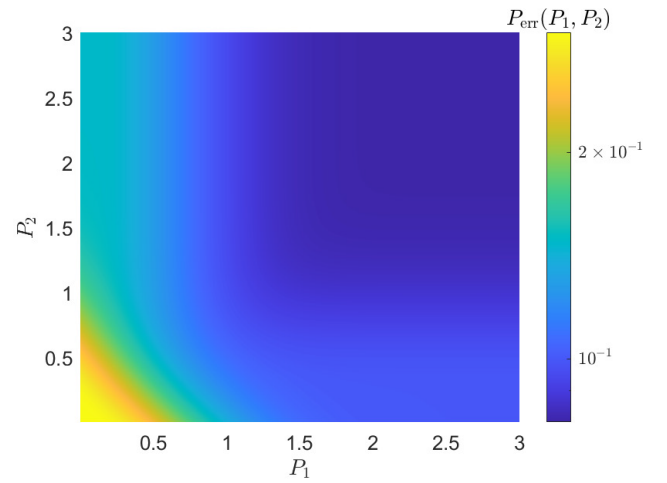


Fig. 8. Error probability as a function of P_1 and P_2 in Case II ($p_1 = 0.3$, $\epsilon_1 = 0.1$, $\epsilon_2 = 0.15$, $N_0 = 1$).

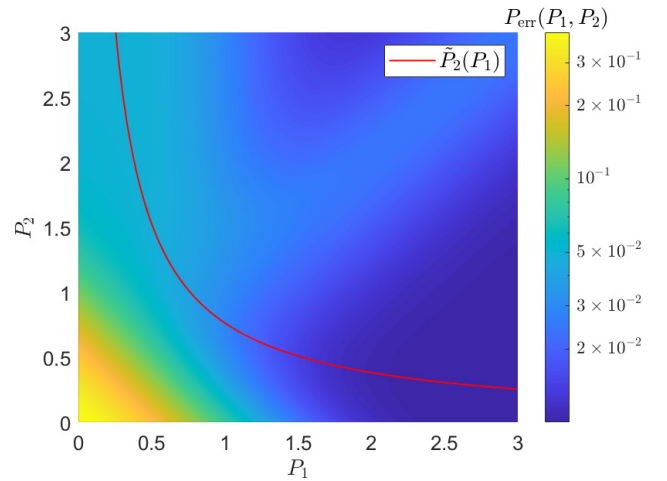


Fig. 9. Error probability as a function of P_1 and P_2 in Case III ($p_1 = 0.4$, $\epsilon_1 = 0.01$, $\epsilon_2 = 0.05$, $N_0 = 1$).

error probability decreases with P_1 , which reinforces exactly the same optimal power allocation as proven. For example, if $P_1^{\max} = P_2^{\max} = 1$, then reading Fig. 9 shows the optimal power allocations are $P_1^* = 1$ and $P_2^* = \tilde{P}_2(1) \approx 0.76$.

Next, we show how the optimal error probability changes with respect to the sensor noise parameters, ϵ_1 and ϵ_2 . We fix the other parameters, p_1, N_0, P_1^{\max} and P_2^{\max} , then for each pair (ϵ_1, ϵ_2) , choose the constellation power allocations P_1^* and P_2^* . Fig. 10 shows the error probability as function of ϵ_1 and ϵ_2 .

When analyzing Fig. 10, note that referencing Fig. 7b, we can identify the regions of the three cases separated by the same line boundaries. We observe that in the Case I region (upper right corner) the error probability takes a constant value of 0.2, which is also the largest error probability across all regions. In the remaining regions (Cases II and III), it is intuitive that the error probability decreases for smaller values of ϵ_1 and ϵ_2 . A more insightful observation is that the error probability is more sensitive to ϵ_1 than ϵ_2 . Especially in the Case III region, we see that varying ϵ_1 has a much larger impact on the error probability than ϵ_2 . Thus, having one very reliable sensor and one very poor sensor can perform better than two moderately accurate sensors.

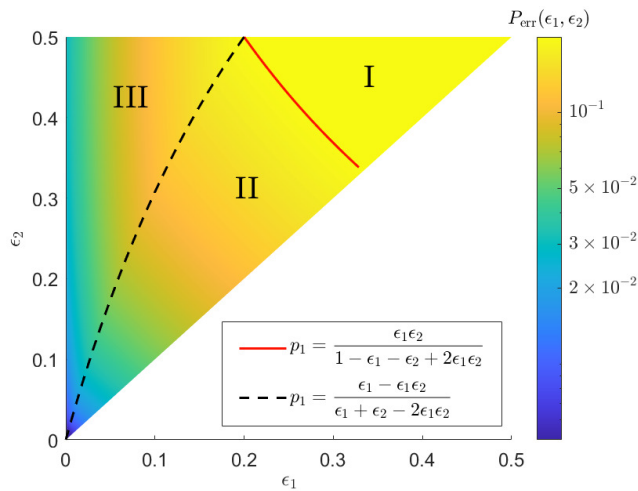


Fig. 10. Error probability as a function of ϵ_1 and ϵ_2 ($p_1 = 0.2$, $P_1^{\max} = 1$, $P_2^{\max} = 1$, $N_0 = 1$). The region and boundary curves for each case are the same as in Fig. 7b.

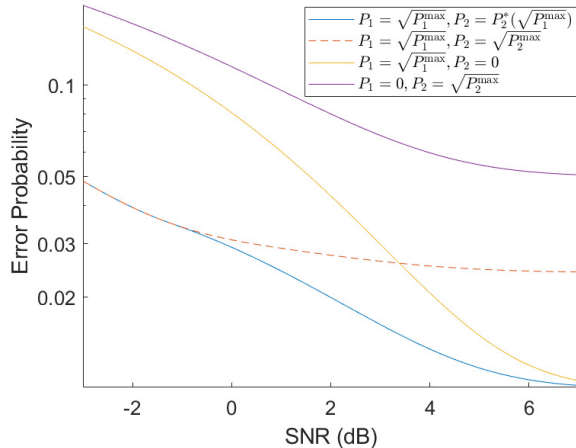


Fig. 11. Error probability as a function of SNR in Case III ($p_1 = 0.4$, $\epsilon_1 = 0.01$, $\epsilon_2 = 0.05$, $P_1^{\max} = 1$, $P_2^{\max} = 1$).

E. Error Probability Vs. Signal to Noise Ratio

To demonstrate this system's SNR response, we vary N_0 to produce various SNR values as defined in (20). We also compare the derived optimal constellation design to other common power allocations. For the following example, the constellations are parameterized by the optimal asymmetric design, $\mathcal{C}_i = \{c_{0,i}, c_{1,i}\} = \{-\beta P_i, \alpha P_i\}$, $i \in 1, 2$. Fig. 11 shows the error probability of various constellation designs in Case III as a function of N_0 , expressed in terms of the SNR.

We make the following observations from this plot. First, at low SNR, the optimal and both max curves are identical. This is because for large enough values of N_0 , $\sqrt{P_2^{\max}} < \tilde{P}_2$ as defined in (3), so $P_2^*(\sqrt{P_1^{\max}}) = \sqrt{P_2^{\max}}$. Next, at high SNR, the optimal and P_1 max curves become asymptotically equal. This is because as $N_0 \rightarrow 0$, $P_2^*(\sqrt{P_1^{\max}}) \rightarrow 0$. At intermediate SNR (around 0-7 dB in this case), the optimal power allocation performs better than any of the alternatives. The largest SNR gain of using the derived optimal constellation is about 2.7 dB, occurring around 0.026 error probability.

VI. CONCLUSION AND FUTURE WORK

In this paper, the optimal one dimensional constellation design for a two sensor binary network was established. After

reducing the problem to a power allocation optimization problem (with the appropriate asymmetric constellation designs from Theorem 1), it was proved that there are distinct cases that arise based on the fixed parameters of the problem, which are p_1 , ϵ_1 and ϵ_2 . In some cases (Cases I and II), the results are intuitive and not unexpected, as the optimal power allocations are to use none or all of the available power. However, in Case III, the most interesting and counter-intuitive result is that the optimal power allocation can be for Sensor 2 (with less correlation to the true data source) to use a portion, but not all of its available power. This is a significant result since Case III is prevalent for many parameter sets of the problem setup. As shown in Fig. 7, Case III becomes the dominant case as the binary source approaches a uniform distribution.

Although this result is theoretically significant, it is also important to consider the following details for any practical implications of this optimization. First, we note that in general, the decision boundaries may not be analytically solvable as they require solving for the roots of (6). This means that it is most feasible to perform the calculations for a specific model of this problem ahead of time, and it would require complex computations to update the model while in use. Further, the optimal power allocation is sensitive to the parameters in the problem, so estimation errors for the parameters of a model could lead to worse performance than using a more robust design, such as using all available power. For this reason, the most practical implementation would be in a case where the optimal error has a large separation from the simpler constellation designs (around 0-5 dB in Fig. 11).

We herein relate our results to more practical problems. First, if there were a sum power constraint instead of individual power constraints (i.e., $P^{\max} = P_1 + P_2$), which applies to systems where sensors are co-located (such as connected motion sensors or powered exoskeleton suits), then we readily obtain that the optimal constellation will be of the form given in this paper, with power allocations $P_1 \leq P^{\max}$ and $P_2 = P_2^*(P_1)$. There is no analytic solution to this optimization, so a numerical computation can be carried to determine the optimal values. Also, even without perfect information about the system parameters, such as p_1 , ϵ_1 , ϵ_2 and N_0 , our results can still be applied with some form of estimates. As seen in Fig. 10, the error probability can have different sensitivities to the ϵ -parameters. The robustness of our optimal signaling scheme can be analyzed when the parameters have estimation errors. Next, if an $N > 2$ sensor network is implemented, our results can be applied iteratively to estimate a good constellation design. Finally, our results show that for distributed detection problems, the typical practice of using all available power is not necessarily optimal, and better error performance can be achieved with less power. This leads to the hypothesis that for problems of this nature, a careful analysis, even just numerically, of the power allocation can yield an improved error performance, while saving power consumption.

To expand further upon our results, the following future directions can be considered. First, a natural extension is to generalize the problem to N sensors ($N \geq 2$), each with their own correlation and power allotments. The analysis becomes increasingly complex for more than two sensors,

so an approximation or bound on error performance could be investigated in some form of pairwise fashion using the results of this paper. Also, sensor network clustering problems such as those found in [22], [23], [24], and [25] could be considered. The performance of a cluster could be approximated using the pairwise expressions derived in this paper. The balance between error probability and energy efficiency could be investigated as a function of cluster organization. Finally, we could consider a sensor network with N sensors, but only two sensors send their data at any given time. The results of this paper could be used to decide which pairs of sensors should be selected, to stay within some power or error constraints.

APPENDIX A PROOF OF THEOREM 2

To prove this theorem, we require multiple intermediate results, which will first be shown. To simplify the notation, we define the following functions of P_1 and P_2 , where \bar{a} , \bar{b} and \bar{c} are as defined in (7).

$$K(P_1) \triangleq \frac{N_0}{2(\alpha + \beta)P_1} \ln \frac{\bar{a}}{-\bar{c}} - \frac{\alpha - \beta}{2} P_1, \quad (21)$$

$$L(P_2) \triangleq \frac{N_0}{2(\alpha + \beta)P_2} \ln \frac{\bar{a}}{-\bar{b}} - \frac{\alpha - \beta}{2} P_2. \quad (22)$$

Note that these are well defined if $\bar{c} \neq 0$ and $\bar{b} \neq 0$, respectively. First, we establish the following relationships which will be applied in various parts of this proof.

Proposition 7: For any $P_1, P_2 > 0$ the following two statements are true if $\bar{b} \neq 0$ and $\bar{c} \neq 0$, respectively:

$$x \underset{\geq}{\leq} \alpha P_1 - L(P_2) \implies ae^{\frac{2(\alpha + \beta)P_2 x}{N_0}} + b \underset{\leq}{\geq} 0, \quad (23)$$

$$x \underset{\geq}{\leq} \alpha P_2 - K(P_1) \implies ae^{\frac{2(\alpha + \beta)P_1 x}{N_0}} + c \underset{\leq}{\geq} 0, \quad (24)$$

where the symbol $\underset{\leq}{\geq}$ means that the statements hold for any of the relations $<$, $>$ or $=$, consistently in the each line.

Proof: We prove (23) using the definition of L from (22). Assume $P_1, P_2 > 0$, $\bar{b} \neq 0$, then if x satisfies

$$\begin{aligned} x &\underset{\geq}{\leq} \alpha P_1 - L(P_2) \\ \implies ae^{\frac{2(\alpha + \beta)P_2 x}{N_0}} + b &\underset{\geq}{\leq} ae^{\frac{2(\alpha + \beta)P_2(\alpha P_1 - L(P_2))}{N_0}} + b, \end{aligned}$$

where

$$\begin{aligned} &ae^{\frac{2(\alpha + \beta)P_2(\alpha P_1 - L(P_2))}{N_0}} + b \\ &= ae^{\frac{2\alpha(\alpha + \beta)P_1 P_2 - 2(\alpha + \beta)P_2 L(P_2)}{N_0}} + b \\ &= ae^{\frac{2\alpha(\alpha + \beta)P_1 P_2 + (\alpha^2 - \beta^2)P_2^2}{N_0} - \ln \frac{\bar{a}}{-\bar{b}}} + b \\ &= -\underbrace{\bar{b}e^{\frac{-(\alpha P_1 - \beta P_2)^2}{N_0}}}_{=b} \underbrace{\frac{a}{\bar{a}}e^{\frac{\alpha^2(P_1 + P_2)^2}{N_0}}}_{=1}} + b \\ &= -b + b = 0. \end{aligned}$$

The proof of (24) is omitted as it follows the same steps as above, using the definition of K from (21). ■

This result is used to determine the properties of the decision boundaries by its influence on the expression in (6), as seen in the following proposition.

Proposition 8: In Case II, for $P_1, P_2 > 0$, if x is the corresponding root of (6), $\bar{b} \neq 0$ and $\bar{c} \neq 0$, then the following

two inequalities hold:

$$x > \alpha P_1 - L(P_2), \quad (25)$$

$$x > \alpha P_2 - K(P_1). \quad (26)$$

Proof: Using Proposition 7, we have

$$x \leq \alpha P_1 - L(P_2) \implies ae^{\frac{2(\alpha + \beta)P_2 x}{N_0}} + b \leq 0 \implies w(x) < 0,$$

$$x \leq \alpha P_2 - K(P_1) \implies ae^{\frac{2(\alpha + \beta)P_1 x}{N_0}} + c \leq 0 \implies w(x) < 0.$$

Hence, x could not be a zero of (6) in either of these cases, showing the desired result. ■

As seen in the above proof, a direct consequence of applying Proposition 7 gives a lower bound on the values of the decision boundary. We also require the following additional result about these lower bounds.

Proposition 9: In Case II, let $\bar{P}_1, P'_1, \bar{P}_2$ and P'_2 be arbitrary real numbers such that $0 < \bar{P}_1 < P'_1$, $0 < \bar{P}_2 < P'_2$. Then the root of (6), x , satisfies the following two inequalities as a function of P_2 and P_1 , respectively:

$$\inf_{P_1 \in [\bar{P}_1, P'_1]} x - \alpha P_1 + L(P_2) > 0, \quad \text{for } \bar{b} \neq 0, P_2 > 0, \quad (27)$$

$$\inf_{P_2 \in [\bar{P}_2, P'_2]} x - \alpha P_2 + K(P_1) > 0, \quad \text{for } \bar{c} \neq 0, P_1 > 0. \quad (28)$$

Proof: To prove (27), let \bar{P}_1 and P'_1 be arbitrary real numbers such that $0 < \bar{P}_1 < P'_1$. For any $P_1 \in [\bar{P}_1, P'_1]$ and $P_2 > 0$, the root of (6), x , satisfies $x - \alpha P_1 + L(P_2) > 0$ from (25) of Proposition 8; therefore

$$\inf_{P_1 \in [\bar{P}_1, P'_1]} x - \alpha P_1 + L(P_2) \geq 0. \quad (29)$$

Next, we define the function

$$w_L(x, P_1) \triangleq ae^{\frac{2(\alpha + \beta)(P_1 + P_2)x}{N_0}} + be^{\frac{2(\alpha + \beta)P_1 x}{N_0}},$$

which is uniformly continuous in both P_1 over $[\bar{P}_1, P'_1]$ and x over $[\alpha \bar{P}_1 - L(P_2), \alpha P'_1 - L(P_2)]$. By (23), $w_L(x, P_1) = 0$ at all points (x, P_1) on the line $x = \alpha P_1 - L(P_2)$. Thus, for any $d' > 0$, there exists $\delta > 0$ such that for any $P_1 \in [\bar{P}_1, P'_1]$ and x that satisfies

$$\alpha P_1 - L(P_2) < x < \alpha P_1 - L(P_2) + \delta, \quad (30)$$

we have

$$w_L(x, P_1) < d'.$$

If (29) holds with equality, then there exists $P_1 \in [\bar{P}_1, P'_1]$ with corresponding root of (6), x , that satisfies (30). In particular, for $d' = -\bar{d}e^{-\frac{\beta^2(P'_1 + P_2)^2}{N_0}}$, which is a positive constant with respect to P_1 and x , we obtain

$$ae^{\frac{2(\alpha + \beta)(P_1 + P_2)x}{N_0}} + be^{\frac{2(\alpha + \beta)P_1 x}{N_0}} < -\bar{d}e^{-\frac{\beta^2(P'_1 + P_2)^2}{N_0}} < -d$$

$$\implies ae^{\frac{2(\alpha + \beta)(P_1 + P_2)x}{N_0}} + be^{\frac{2(\alpha + \beta)P_1 x}{N_0}} + d < 0$$

$$\implies w(x) < 0,$$

where the last inequality holds because $c < 0$ in the expression of $w(x)$ in (6) for Case II. This contradicts x being the root of (6), completing the proof. The proof of (28) is omitted as it follows the same steps as above. ■

This result shows that the decision boundary is bounded away from the lower bound over any finite interval of power allocation. This is a small, but essential result for the main proof as it guarantees that the sequence of powers we use will grow large enough to reach the necessary value.

Using Propositions 7, 8 and 9, we will prove Theorem 2 by showing the following two statements:

- 1) If $0 < P_1 < P'_1, 0 < P_2$, then $P_{\text{err}}(P_1, P_2) > P_{\text{err}}(P'_1, P_2)$
- 2) If $0 < P_1, 0 < P_2 < P'_2$, then $P_{\text{err}}(P_1, P_2) > P_{\text{err}}(P_1, P'_2)$

To show Statement 1, fix $0 < P_1 < P'_1, 0 < P_2$. Let x and x' be the roots of (6) corresponding to the pairs (P_1, P_2) and (P'_1, P_2) , respectively. We define the following sequence $\{P_{1,i}\}_{i=0}^{\infty}$ recursively.

$$P_{1,0} = P_1, P_{1,i+1} = \begin{cases} P'_1, & \bar{b} = 0 \\ \frac{1}{\alpha}(x_i + L(P_2)), & \bar{b} \neq 0 \end{cases}$$

where x_i is the root to (6) corresponding to $P_{1,i}$, \bar{b} is from (7) and L is as defined in (22). Note that if $\bar{b} \neq 0$ and $P_{1,i} < P'_1$, applying (27) from Proposition 9 gives

$$\begin{aligned} P_{1,i+1} - P_{1,i} &= \frac{1}{\alpha}(x_i + L(P_2)) - P_{1,i} \\ &\geq \frac{1}{\alpha} \inf_{P_1 \in [P_1, P'_1]} \bar{x} - \alpha \bar{P}_1 + L(P_2) \stackrel{(27)}{>} 0, \end{aligned}$$

where \bar{x} denotes the root of (6) for (\bar{P}_1, P_2) . This shows that the sequence $\{P_{1,i}\}_{i=0}^{\infty}$ increases by at least this constant if $P_{1,i} < P'_1$. Therefore there exists i' large enough such that $P_{1,i'} \geq P'_1$. Hence, it is sufficient to show that for all i

$$P_{\text{err}}(P_{1,i}, P_2) - P_{\text{err}}(P_{1,i+1}, P_2) > 0.$$

Using the upper bound in Proposition 3, it is sufficient to show

$$\begin{aligned} P_{\text{err}}(P_{1,i}, P_2) - P_{\text{err},x_i}^{\text{UB}}(P_{1,i+1}, P_2) &> 0 \\ \iff P_{\text{err},x_i}^{\text{UB}}(P_{1,i}, P_2) - P_{\text{err},x_i}^{\text{UB}}(P_{1,i+1}, P_2) &> 0, \end{aligned}$$

since $P_{\text{err}}(P_{1,i}, P_2) = P_{\text{err},x_i}^{\text{UB}}(P_{1,i}, P_2)$ by its definition.

It is now sufficient to show $P_{\text{err},x_i}^{\text{UB}}$ is decreasing in P_1 over $(P_{1,i}, P_{1,i+1})$. The derivative of this expression is:

$$\begin{aligned} \frac{dP_{\text{err},x_i}^{\text{UB}}}{dP_1} &= \frac{-1}{\sigma\sqrt{2\pi}} e^{-\frac{x_i^2}{N_0}} \left(\alpha \left(a e^{\frac{2\alpha(P_1+P_2)x_i}{N_0}} + b e^{\frac{2(\alpha P_1 - \beta P_2)x_i}{N_0}} \right) \right. \\ &\quad \left. - \beta \left(c e^{\frac{2(-\beta P_1 + \alpha P_2)x_i}{N_0}} + d e^{\frac{-2\beta(P_1+P_2)x_i}{N_0}} \right) \right). \end{aligned} \quad (31)$$

If $\bar{b} = 0$, this derivative is negative for any P_1 (since this is equivalent to $b = 0$). If $\bar{b} \neq 0$, then we apply (23) from Proposition 7 and conclude that

$$\begin{aligned} P_1 < P_{1,i+1} &= \frac{1}{\alpha}(x_i + L(P_2)) \\ \iff x_i &> \alpha P_1 - L(P_2) \\ \implies a e^{\frac{2(\alpha+\beta)P_2 x_i}{N_0}} + b &> 0 \\ \implies a e^{\frac{2\alpha(P_1+P_2)x_i}{N_0}} + b e^{\frac{2(\alpha P_1 - \beta P_2)x_i}{N_0}} &> 0 \\ \implies \frac{dP_{\text{err},x_i}^{\text{UB}}}{dP_1} &< 0. \end{aligned}$$

The proof of Statement 2 is omitted as it follows the exact same steps as above, replacing the roles of $L(P_2)$ with $K(P_1)$, \bar{b} with \bar{c} , and applying (24) and (28) instead of (23) and (27). ■

APPENDIX B

PROOF OF THEOREM 3

First, we define the following two functions of x , for any fixed P_1 and P_2 :

$$\begin{aligned} g(x) &\triangleq (p_1 p_{11|1} - p_0 p_{11|0}) Q\left(\frac{\alpha P_1 + \alpha P_2 - x}{\sigma}\right) \\ &\quad + (p_1 p_{01|1} - p_0 p_{01|0}) Q\left(\frac{-\beta P_1 + \alpha P_2 - x}{\sigma}\right), \\ h(x) &\triangleq (p_1 p_{10|1} - p_0 p_{10|0}) Q\left(\frac{\alpha P_1 - \beta P_2 - x}{\sigma}\right) \\ &\quad + (p_1 p_{00|1} - p_0 p_{00|0}) Q\left(\frac{-\beta P_1 - \beta P_2 - x}{\sigma}\right). \end{aligned}$$

These functions are significant because they decompose the error expression. For example, if P_1 and P_2 are fixed with a unique corresponding root of (6), x , the error probability can be written as

$$P_{\text{err}}(P_1, P_2) = g(x) + h(x) + \sum_{(l,m) \in \{0,1\}^2} p_0 p_{lm|0}.$$

Further, they have the following unique minimizers with analytic expressions corresponding to the bounds given in Proposition 5.

Proposition 10: In Case III, for any $P_1, P_2 > 0$, $g(x)$ is minimized at $x = \alpha P_2 - K_\alpha(P_1)$ and $h(x)$ is minimized at $x = -\beta P_2 + K_\beta(P_1)$.

Proof: Let $P_1, P_2 > 0$. The following are expressions for the derivatives:

$$\begin{aligned} \frac{dg}{dx} &= \frac{1}{\sigma\sqrt{2\pi}} e^{-\frac{x^2}{N_0}} \left(a e^{\frac{2\alpha(P_1+P_2)x}{N_0}} + c e^{\frac{2(-\beta P_1 + \alpha P_2)x}{N_0}} \right) \\ \frac{dh}{dx} &= \frac{1}{\sigma\sqrt{2\pi}} e^{-\frac{x^2}{N_0}} \left(b e^{\frac{2(\alpha P_1 - \beta P_2)x}{N_0}} + d e^{\frac{-2\beta(P_1+P_2)x}{N_0}} \right). \end{aligned}$$

Next, we apply the results of Proposition 4 to show

$$\begin{aligned} x \leq \alpha P_2 - K_\alpha(P_1) &\implies 0 \geq a e^{\frac{2(\alpha+\beta)P_1 x}{N_0}} + c \\ \implies 0 &\geq a e^{\frac{2\alpha(P_1+P_2)x}{N_0}} + c e^{\frac{2(-\beta P_1 + \alpha P_2)x}{N_0}} \\ \implies 0 &\geq \frac{dg}{dx}, \end{aligned}$$

and

$$\begin{aligned} x \leq -\beta P_2 + K_\beta(P_1) &\implies 0 \geq b e^{\frac{2(\alpha+\beta)P_1 x}{N_0}} + d \\ \implies 0 &\geq b e^{\frac{2(\alpha P_1 - \beta P_2)x}{N_0}} + d e^{\frac{-2\beta(P_1+P_2)x}{N_0}} \\ \implies 0 &\geq \frac{dh}{dx}. \end{aligned}$$

Now fix $P_1 > 0$. Let \tilde{a}_{lm} be the constellation points and \tilde{x} be the root of (6) corresponding to P_1 and $\tilde{P}_2(P_1)$. Let $P_2 \neq \tilde{P}_2(P_1)$. Let a_{lm} be the constellation points and \mathcal{X} denote the set of roots of (6) corresponding to P_1 and P_2 . ■

First we analyze the case where $|\mathcal{X}| = 1$. Let $\mathcal{X} = \{x\}$. In this case, the error expression, $P_{\text{er}}(P_1, P_2)$, will have the same form as given in (8). Also, since there is a unique root, \tilde{x} , at $\tilde{P}_2(P_1)$, $P_{\text{er}}(P_1, \tilde{P}_2(P_1))$ takes the form of (8) as well. Therefore, we must show

$$\begin{aligned} & \sum_{(l,m) \in \{0,1\}^2} (p_1 p_{lm|1} - p_0 p_{lm|0}) Q\left(\frac{\tilde{a}_{lm} - \tilde{x}}{\sigma}\right) < \\ & \sum_{(l,m) \in \{0,1\}^2} (p_1 p_{lm|1} - p_0 p_{lm|0}) Q\left(\frac{a_{lm} - x}{\sigma}\right) \\ \iff & g(\alpha P_2 - K_\alpha(P_1)) + h(-\beta P_2 + K_\beta(P_1)) < \\ & g(x) + h(x). \end{aligned}$$

This result follows immediately by applying Proposition 10, since $x \neq \alpha P_2 - K_\alpha(P_1)$ and $x \neq -\beta P_2 + K_\beta(P_1)$ for $P_2 \neq \tilde{P}_2(P_1)$ from Proposition 5.

For the case that $|\mathcal{X}| = 3$, we represent this as $\mathcal{X} = \{x_1, x_2, x_3\}$ such that $x_1 < x_2 < x_3$. In this case, the error probability takes the form of (17), noting that it can be expressed in terms of g and h :

$$\begin{aligned} & P_{\text{er}}(P_1, P_2) \\ &= \sum_{(l,m) \in \{0,1\}^2} (p_1 p_{lm|1} - p_0 p_{lm|0}) \left(Q\left(\frac{a_{lm} - x_1}{\sigma}\right) \right. \\ & \quad \left. - Q\left(\frac{a_{lm} - x_2}{\sigma}\right) + Q\left(\frac{a_{lm} - x_3}{\sigma}\right) \right) + p_0 p_{lm|0}, \\ &= g(x_1) - g(x_2) + g(x_3) \\ & \quad + h(x_1) - h(x_2) + h(x_3) + \sum_{(l,m) \in \{0,1\}^2} p_0 p_{lm|0}. \end{aligned}$$

Hence we must show

$$\begin{aligned} & g(\alpha P_2 - K_\alpha(P_1)) + h(-\beta P_2 + K_\beta(P_1)) \\ & < g(x_1) - g(x_2) + g(x_3) + h(x_1) - h(x_2) + h(x_3). \end{aligned} \quad (32)$$

First note that by applying Proposition 10, we have

$$g(\alpha P_2 - K_\alpha(P_1)) + h(-\beta P_2 + K_\beta(P_1)) < g(x_3) + h(x_1). \quad (33)$$

Now we will show

$$g(x_1) - g(x_2) + h(x_3) - h(x_2) \geq 0. \quad (34)$$

Since $|\mathcal{X}| = 3$ we can infer that $P_2 > \tilde{P}_2(P_1)$ by taking the contra-positive of Proposition 6. Then we can apply Proposition 5 which implies $x_2 \in (-\beta P_2 + K_\beta(P_1), \alpha P_2 - K_\alpha(P_1))$. Finally, applying the same derivative analysis as in Proposition 10 shows that $g(x)$ is decreasing on $[x_1, x_2]$ and $h(x)$ is increasing on $[x_2, x_3]$. This implies (34). Combining (33) with (34) implies (32). ■

APPENDIX C

PROOF OF THEOREM 4

We follow similar steps to the proof of Theorem 2, with more complex steps because there are two bounding lines to account for in Case III. First, we must use the following intermediate result about the bounds on the decision boundaries.

Proposition 11: In Case III, for any $P_1 > 0$, let \bar{P}_2 and P'_2 be arbitrary real numbers such that $0 < \bar{P}_2 < P'_2 < \tilde{P}_2(P_1)$, where $\tilde{P}_2(P_1)$ is as defined in (11). Then the root of (6), x , satisfies the following two inequalities:

$$\inf_{P_2 \in [\bar{P}_2, P'_2]} x - \alpha P_2 + K_\alpha(P_1) > 0, \quad (35)$$

$$\inf_{P_2 \in [\bar{P}_2, P'_2]} K_\beta(P_1) - \beta P_2 - x > 0. \quad (36)$$

Proof: The details are omitted as it follows the same steps as the proof of Proposition 9. ■

Now, fix $0 < P_1$, $0 < P_2 < P'_2 < \tilde{P}_2$. Let x and x' be the roots of (6) corresponding to P_2 and P'_2 , respectively. We define the following sequence $\{P_{2,i}\}_{i=0}^\infty$ recursively.

$$P_{2,0} = P_2,$$

$$P_{2,i+1} = \min\left(\frac{1}{\alpha}(x_i + K_\alpha(P_1)), \frac{1}{\beta}(K_\beta(P_1) - x_i)\right),$$

where x_i is the root of (6) corresponding to $P_{2,i}$. Note that (16) implies $P_{2,i} \leq \tilde{P}_2$ for any $i \geq 0$, so there is always a unique x_i . If $P_{2,i} < P'_2$, applying (35) and (36) means one of the following two statements must be true:

$$\begin{aligned} P_{2,i+1} - P_{2,i} &= \frac{1}{\alpha}(x_i + K_\alpha(P_1)) - P_{2,i} \\ &\geq \underbrace{\frac{1}{\alpha} \inf_{\bar{P}_2 \in [P_2, P'_2]} \bar{x} - \alpha \bar{P}_2 + K_\alpha(P_1)}_{\triangleq K'_\alpha} > 0, \end{aligned} \quad (35)$$

or

$$\begin{aligned} P_{2,i+1} - P_{2,i} &= \frac{1}{\beta}(K_\beta(P_1) - x_i) - P_{2,i} \\ &\geq \underbrace{\frac{1}{\beta} \inf_{\bar{P}_2 \in [P_2, P'_2]} K_\beta(P_1) - \beta \bar{P}_2 - \bar{x}}_{\triangleq K'_\beta} > 0, \end{aligned} \quad (36)$$

so

$$P_{2,i+1} - P_{2,i} \geq \min(K'_\alpha, K'_\beta) > 0.$$

where \bar{x} denotes the root of (6) for (P_1, \bar{P}_2) . This means that the sequence $\{P_{2,i}\}_{i=0}^\infty$ increases by at least this fixed constant if $P_{2,i} < P'_2$. Therefore, there exists i' large enough such that $P_{2,i'} \geq P'_2$. Hence, it is sufficient to show that for all i

$$P_{\text{er}}(P_1, P_{2,i}) - P_{\text{er}}(P_1, P_{2,i+1}) > 0.$$

Using the upper bound in Proposition 3 (which is valid for exactly the same reasons as before), it is sufficient to show

$$\begin{aligned} & P_{\text{er}}(P_1, P_{2,i}) - P_{\text{er},x_i}^{\text{UB}}(P_1, P_{2,i+1}) > 0 \\ \iff & P_{\text{er},x_i}^{\text{UB}}(P_1, P_{2,i}) - P_{\text{er},x_i}^{\text{UB}}(P_1, P_{2,i+1}) > 0, \end{aligned}$$

since $P_{\text{er}}(P_1, P_{2,i}) = P_{\text{er},x_i}^{\text{UB}}(P_1, P_{2,i})$ by definition in (9). It is now sufficient to show $P_{\text{er},x_i}^{\text{UB}}$ is decreasing in P_2 over $(P_{2,i}, P_{2,i+1})$. We have

$$\begin{aligned} \frac{dP_{\text{er},x_i}^{\text{UB}}}{dP_2} &= \frac{-1}{\sigma\sqrt{2\pi}} e^{-\frac{x_i^2}{N_0}} \left(\alpha \left(a e^{\frac{2\alpha(P_1+P_2)x_i}{N_0}} + c e^{\frac{2(-\beta P_1+\alpha P_2)x_i}{N_0}} \right) \right. \\ & \quad \left. - \beta \left(b e^{\frac{2(\alpha P_1-\beta P_2)x_i}{N_0}} + d e^{\frac{-2\beta(P_1+P_2)x_i}{N_0}} \right) \right), \end{aligned}$$

where applying Proposition 4 gives

$$\begin{aligned} P_2 < P_{2,i+1} &\leq \frac{1}{\alpha}(x_i + K_\alpha(P_1)) \\ \implies x_i &> \alpha P_2 - K_\alpha(P_1) \\ \implies 0 &< ae^{\frac{2(\alpha+\beta)P_1 x_i}{N_0}} + c \\ \implies 0 &< ae^{\frac{2\alpha(P_1+P_2)x_i}{N_0}} + ce^{\frac{2(-\beta P_1+\alpha P_2)x_i}{N_0}}, \end{aligned}$$

and

$$\begin{aligned} P_2 < P_{2,i+1} &\leq \frac{1}{\beta}(K_\beta(P_1) - x_i) \\ \implies x_i &< -\beta P_2 + K_\beta(P_1) \\ \implies 0 &> be^{\frac{2(\alpha+\beta)P_1 x_i}{N_0}} + d \\ \implies 0 &> be^{\frac{2(\alpha P_1 - \beta P_2)x_i}{N_0}} + de^{\frac{-2\beta(P_1+P_2)x_i}{N_0}}, \end{aligned}$$

so

$$\implies \frac{dP_{\text{err},x_i}^{\text{UB}}}{dP_2} < 0.$$

■

APPENDIX D PROOF OF THEOREM 5

Let $P_1 > 0$. We can express the optimal power allocation for P_2 as the following function of P_1 :

$$P_2^*(P_1) = \begin{cases} \sqrt{P_2^{\text{max}}} & P_1 < P_1^{\text{thresh}} \\ \tilde{P}_2(P_1) & P_1 \geq P_1^{\text{thresh}} \end{cases}$$

where

$$P_1^{\text{thresh}} \triangleq \frac{N_0}{2(\alpha+\beta)^2 \sqrt{P_2^{\text{max}}}} \ln \frac{\bar{a}\bar{d}}{\bar{b}\bar{c}}.$$

We analyze this in two cases. First, assume $P_1 < P_1^{\text{thresh}}$. Since $P_2^*(P_1) = \sqrt{P_2^{\text{max}}} < \tilde{P}_2(P_1)$, Proposition 6 implies that there is a unique root, x , to (6) corresponding to P_1 and P_2 . Hence, by the same reasoning as in Theorem 2 it is sufficient to show $P_{\text{err},x}^{\text{UB}}$ is decreasing in P_1 . Unlike the previous proof, we can see immediately from the expression given in (31) that this derivative is negative for all P_1 because $\bar{b} > 0$ in Case III. Next, for $P_1 \geq P_1^{\text{thresh}}$ we have

$$P_2^*(P_1) = \frac{N_0}{2(\alpha+\beta)^2 P_1} \ln \frac{\bar{a}\bar{d}}{\bar{b}\bar{c}}.$$

Let x^* be the root to (6) for P_1 and $P_2^*(P_1)$. (16) implies $x^* = \alpha P_2^*(P_1) - K_\alpha(P_1) = -\beta P_2^*(P_1) + K_\beta(P_1)$. Substituting these relationships into the expression for the error probability given in (8) yields

$$\begin{aligned} P_{\text{err}}(P_1, P_2^*(P_1)) &= \bar{a}Q\left(\frac{1}{\sigma}\left(\alpha P_1 + P_a - \frac{\alpha - \beta}{2}P_1\right)\right) \\ &+ \bar{c}Q\left(\frac{1}{\sigma}\left(-\beta P_1 + P_a - \frac{\alpha - \beta}{2}P_1\right)\right) \\ &+ \bar{b}Q\left(\frac{1}{\sigma}\left(\alpha P_1 - P_b - \frac{\alpha - \beta}{2}P_1\right)\right) \end{aligned}$$

$$\begin{aligned} &+ \bar{d}Q\left(\frac{1}{\sigma}\left(-\beta P_1 - P_b - \frac{\alpha - \beta}{2}P_1\right)\right) \\ &+ \sum_{(l,m) \in \{0,1\}^2} p_0 p_{lm|0}, \end{aligned}$$

where we define

$$P_a \triangleq \frac{N_0}{2(\alpha+\beta)P_1} \ln \frac{\bar{a}}{-\bar{c}}, \quad P_b \triangleq \frac{N_0}{2(\alpha+\beta)P_1} \ln \frac{-\bar{d}}{\bar{b}},$$

noting that

$$\frac{dP_a}{dP_1} = -\frac{P_a}{P_1}, \quad \frac{dP_b}{dP_1} = -\frac{P_b}{P_1}.$$

Then derivative analysis on the error probability yields

$$\begin{aligned} \frac{dP_{\text{err}}}{dP_1} &= -\frac{1}{\sigma\sqrt{2\pi}} \left(\left(\frac{\alpha+\beta}{2} - \frac{P_a}{P_1} \right) \bar{a}e^{\frac{-(\frac{\alpha+\beta}{2}P_1+P_a)^2}{N_0}} \right. \\ &+ \left(-\frac{\alpha+\beta}{2} - \frac{P_a}{P_1} \right) \bar{c}e^{\frac{-(-\frac{\alpha+\beta}{2}P_1+P_a)^2}{N_0}} \\ &+ \left(\frac{\alpha+\beta}{2} + \frac{P_b}{P_1} \right) \bar{b}e^{\frac{-(\frac{\alpha+\beta}{2}P_1-P_b)^2}{N_0}} \\ &+ \left. \left(-\frac{\alpha+\beta}{2} + \frac{P_b}{P_1} \right) \bar{d}e^{\frac{-(\frac{\alpha+\beta}{2}P_1+P_b)^2}{N_0}} \right) \\ &= -\frac{e^{\frac{-(\frac{\alpha+\beta}{2}P_1)^2}{N_0}}}{\sigma\sqrt{2\pi}} \left(e^{\frac{-P_a^2}{N_0}} \left(\left(\frac{\alpha+\beta}{2} - \frac{P_a}{P_1} \right) \bar{a}e^{\frac{-(\alpha+\beta)P_1 P_a}{N_0}} \right. \right. \\ &+ \left. \left(-\frac{\alpha+\beta}{2} - \frac{P_a}{P_1} \right) \bar{c}e^{\frac{(\alpha+\beta)P_1 P_a}{N_0}} \right) \\ &+ e^{\frac{-P_b^2}{N_0}} \left(\left(\frac{\alpha+\beta}{2} + \frac{P_b}{P_1} \right) \bar{b}e^{\frac{(\alpha+\beta)P_1 P_b}{N_0}} \right. \\ &+ \left. \left. \left(-\frac{\alpha+\beta}{2} + \frac{P_b}{P_1} \right) \bar{d}e^{\frac{-(\alpha+\beta)P_1 P_b}{N_0}} \right) \right) \\ &= -\frac{e^{\frac{-(\frac{\alpha+\beta}{2}P_1)^2}{N_0}}}{\sigma\sqrt{2\pi}} \left(e^{\frac{-P_a^2}{N_0}} \left(\left(\frac{\alpha+\beta}{2} - \frac{P_a}{P_1} \right) \sqrt{-\bar{a}\bar{c}} \right. \right. \\ &- \left. \left(-\frac{\alpha+\beta}{2} - \frac{P_a}{P_1} \right) \sqrt{-\bar{a}\bar{c}} \right) \\ &+ e^{\frac{-P_b^2}{N_0}} \left(\left(\frac{\alpha+\beta}{2} + \frac{P_b}{P_1} \right) \sqrt{-\bar{b}\bar{d}} \right. \\ &- \left. \left. \left(-\frac{\alpha+\beta}{2} + \frac{P_b}{P_1} \right) \sqrt{-\bar{b}\bar{d}} \right) \right) \\ &= -\frac{\alpha+\beta}{\sigma\sqrt{2\pi}} e^{\frac{-(\frac{\alpha+\beta}{2}P_1)^2}{N_0}} \left(e^{\frac{-P_a^2}{N_0}} \sqrt{-\bar{a}\bar{c}} + e^{\frac{-P_b^2}{N_0}} \sqrt{-\bar{b}\bar{d}} \right) \\ &< 0. \end{aligned}$$

■

REFERENCES

- [1] L. Sardellitti, G. Takahara, and F. Alajaji, "Optimized distributed detection over a two sensor binary Gaussian MAC network," in *Proc. Can. Conf. Electr. Comput. Eng. (CCECE)*, 2024, pp. 1–2.
- [2] W. Li and H. Dai, "Distributed detection in wireless sensor networks using a multiple access channel," *IEEE Trans. Signal Process.*, vol. 55, no. 3, pp. 822–833, Mar. 2007.

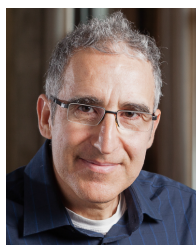
- [3] X. Guo, Y. He, S. Atapattu, S. Dey, and J. S. Evans, "Power allocation for distributed detection systems in wireless sensor networks with limited fusion center feedback," *IEEE Trans. Commun.*, vol. 66, no. 10, pp. 4753–4766, Oct. 2018.
- [4] H. Jeffreys, "An invariant form for the prior probability in estimation problems," *Proc. Roy. Soc. London. Ser. A, Math. Phys. Sci.*, vol. 186, no. 1007, pp. 453–461, 1946.
- [5] C. Tepedelenlioglu and S. Dasarathan, "Distributed detection over Gaussian multiple access channels with constant modulus signaling," *IEEE Trans. Signal Process.*, vol. 59, no. 6, pp. 2875–2886, Jun. 2011.
- [6] S. Dasarathan and C. Tepedelenlioglu, "Distributed estimation and detection with bounded transmissions over Gaussian multiple access channels," *IEEE Trans. Signal Process.*, vol. 62, no. 13, pp. 3454–3463, Sep. 2014.
- [7] G. Ferrari, M. Martalò, and A. Abrardo, "Information fusion in wireless sensor networks with source correlation," *Inf. Fusion*, vol. 15, pp. 80–89, Jan. 2014.
- [8] S. R. Panigrahi, N. Björnsell, and M. Bengtsson, "Data fusion in the air with non-identical wireless sensors," *IEEE Trans. Signal Inf. Process. Over Netw.*, vol. 5, no. 4, pp. 646–656, Dec. 2019.
- [9] R. Jiang and B. Chen, "Fusion of censored decisions in wireless sensor networks," *IEEE Trans. Wireless Commun.*, vol. 4, no. 6, pp. 2668–2673, Nov. 2005.
- [10] M. Gastpar, "Uncoded transmission is exactly optimal for a simple Gaussian 'sensor' network," *IEEE Trans. Inf. Theory*, vol. 54, no. 11, pp. 5247–5251, Oct. 2008.
- [11] H. Behroozi, F. Alajaji, and T. Linder, "On the optimal performance in asymmetric Gaussian wireless sensor networks with fading," *IEEE Trans. Signal Process.*, vol. 58, no. 4, pp. 2436–2441, Apr. 2010.
- [12] J.-J. Weng, F. Alajaji, and T. Linder, "Optimized signaling of binary correlated sources over Gaussian multiple access channels," in *Proc. IEEE 88th Veh. Technol. Conf. (VTC-Fall)*, Aug. 2018, pp. 1–5.
- [13] C.-H. Lin, S.-L. Shieh, T.-C. Chi, and P.-N. Chen, "Optimal inter-constellation rotation based on minimum distance criterion for uplink NOMA," *IEEE Trans. Veh. Technol.*, vol. 68, no. 1, pp. 525–539, Jan. 2019.
- [14] H.-P. Liu, S.-L. Shieh, C.-H. Lin, and P.-N. Chen, "A minimum distance criterion based constellation design for uplink NOMA," in *Proc. IEEE 90th Veh. Technol. Conf. (VTC-Fall)*, Sep. 2019, pp. 1–5.
- [15] K.-H. Ngo, S. Yang, M. Guillaud, and A. Decurninge, "Joint constellation design for noncoherent MIMO multiple-access channels," *IEEE Trans. Inf. Theory*, vol. 68, no. 11, pp. 7281–7305, Nov. 2022.
- [16] B. K. Ng and C.-T. Lam, "Joint power and modulation optimization in two-user non-orthogonal multiple access channels: A minimum error probability approach," *IEEE Trans. Veh. Technol.*, vol. 67, no. 11, pp. 10693–10703, Nov. 2018.
- [17] G. Takahara, F. Alajaji, N. C. Beaulieu, and H. Kuai, "Constellation mappings for two-dimensional signaling of nonuniform sources," *IEEE Trans. Commun.*, vol. 51, no. 3, pp. 400–408, Mar. 2003.
- [18] B. Moore, G. Takahara, and F. Alajaji, "Pairwise optimization of modulation constellations for non-uniform sources," *Can. J. Electr. Comput. Eng.*, vol. 34, no. 4, pp. 167–177, Fall. 2009.
- [19] S. Vlajkov, A. Jovanović, and Z. Perić, "Approach in companding-quantisation-inspired PAM constellation design," *IET Commun.*, vol. 12, no. 18, pp. 2305–2314, Nov. 2018.
- [20] L. Wei, "Optimized M-ary orthogonal and bi-orthogonal signaling using coherent receiver with non-equal symbol probabilities," *IEEE Commun. Lett.*, vol. 16, no. 6, pp. 793–796, Jun. 2012.
- [21] G. J. O. Jameson, "Counting zeros of generalised polynomials: Descartes' rule of signs and Laguerre's extensions," *Math. Gazette*, vol. 90, no. 518, pp. 223–234, Jul. 2006.
- [22] S. Yi, J. Heo, Y. Cho, and J. Hong, "PEACH: Power-efficient and adaptive clustering hierarchy protocol for wireless sensor networks," *Comput. Commun.*, vol. 30, nos. 14–15, pp. 2842–2852, Oct. 2007.
- [23] E. Pei, J. Pei, S. Liu, W. Cheng, Y. Li, and Z. Zhang, "A heterogeneous nodes-based low energy adaptive clustering hierarchy in cognitive radio sensor network," *IEEE Access*, vol. 7, pp. 132010–132026, 2019.
- [24] G. Chen, F. G. Nocetti, J. S. Gonzalez, and I. Stojmenovic, "Connectivity based k-hop clustering in wireless networks," in *Proc. 35th Annu. Hawaii Int. Conf. Syst. Sci.*, Jan. 2002, pp. 2450–2459.
- [25] A. Bendjeddou, H. Laoufi, and S. Boudjit, "LEACH-S: Low energy adaptive clustering hierarchy for sensor network," in *Proc. Int. Symp. Netw., Comput. Commun. (ISNCC)*, Jun. 2018, pp. 1–6.



Luca Sardellitti received the B.A.Sc. and M.A.Sc. degrees in applied mathematics and engineering from Queen's University, Canada, in 2022 and 2024, respectively. His research interests include sensor networks, distributed detection, and signaling design.



Glen Takahara (Member, IEEE) received the B.A. degree (Hons.) in mathematics, with a specialization in statistics from The University of British Columbia in 1989, and the M.Sc. and Ph.D. degrees in statistics from Carnegie Mellon University, in 1990 and 1994, respectively. In 1993, he joined the Department of Mathematics and Statistics, Queen's University, Kingston, ON, Canada, where he is currently an Associate Professor of statistics. His research interests include spectral analysis of time series, signal processing, Bayesian methods, vehicular networks, channel modeling, and population health statistics.



Fady Alajaji (Senior Member, IEEE) received the B.E. degree (Hons.) in electrical engineering from the American University of Beirut, Lebanon, in 1988, and the M.Sc. and Ph.D. degrees in electrical engineering from the University of Maryland, College Park, in 1990 and 1994, respectively.

In 1994, he held a post-doctoral appointment with the Institute for Systems Research, University of Maryland. In 1995, he joined the Department of Mathematics and Statistics, Queen's University, Kingston, ON, Canada, where he is currently a Professor of mathematics and engineering. Since 1997, he has been cross-appointed with the Department of Electrical and Computer Engineering, Queen's University. From 2013 to 2014, he was the Acting Head of the Department of Mathematics and Statistics. From 2003 to 2008 and from 2018 to 2019, he was the Chair of the Queen's Mathematics and Engineering Program. His research interests include information theory, digital communications, error control coding, data compression, joint source-channel coding, network epidemics, generative adversarial networks, and data privacy and fairness in machine learning. He received the Premiers Research Excellence Award from the Province of Ontario. He served as an organizer and a technical program committee member for several international conferences and workshops. From 2019 to 2022, he was an Associate Editor of Shannon Theory and Information Measures for IEEE TRANSACTIONS ON INFORMATION THEORY, from 2019 to 2022. He served as an Area Editor (2008–2015) for Source-Channel Coding and Signal Processing and an Editor (2003–2012) for Source and Source-Channel Coding for IEEE TRANSACTIONS ON COMMUNICATIONS.